iScience

CellPress

Article

Ventral Hippocampal-Prefrontal Interaction Affects Social Behavior via Parvalbumin Positive Neurons in the Medial Prefrontal Cortex

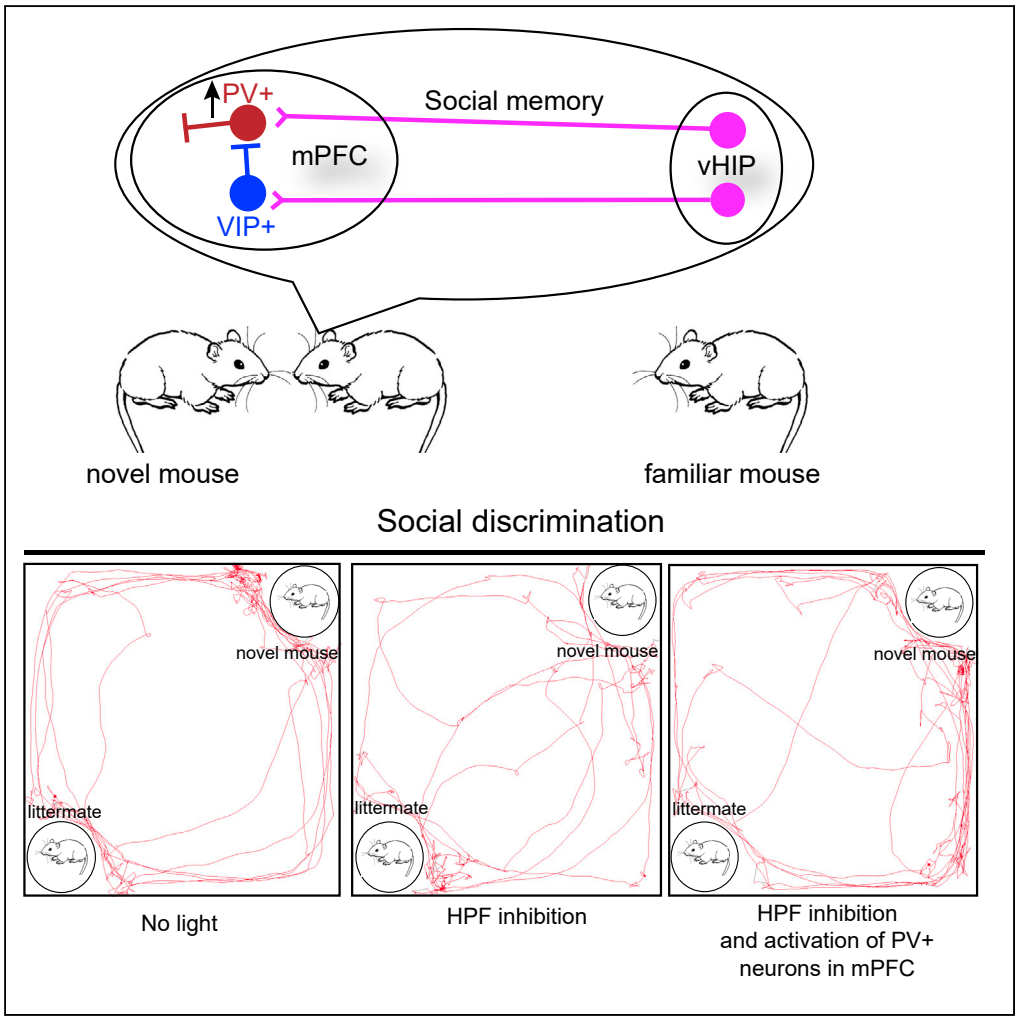

Qingtao Sun, Xiangning Li, Anan Li, Jianping Zhang, Zhangheng Ding, Hui Gong, Qingming Luo

qluo@mail.hust.edu.cn

HIGHLIGHTS

Inhibition of vHIP or direct vHIP-mPFC pathway disrupts social memory expression

Social behaviors preferentially recruit PV+ neurons in mPFC

Activation of PV+ neurons in mPFC rescue the vHIP-related impairment of social memory

Inhibition of VIP+ neurons in mPFC rescue the vHIP-related impairment of social memory

Sun et al., iScience *23*, 100894
March 27, 2020
https://doi.org/10.1016/j.isci.2020.100894

iScience

CellPress

Article

Ventral Hippocampal-Prefrontal Interaction Affects Social Behavior via Parvalbumin Positive Neurons in the Medial Prefrontal Cortex

Qingtao Sun,[1,2,4] Xiangning Li,[1,2,3,4] Anan Li,[1,2,3] Jianping Zhang,[1,2] Zhangheng Ding,[1,2] Hui Gong,[1,2,3] and Qingming Luo[1,2,3,5,*]

SUMMARY

Ventral hippocampus (vHIP) and medial prefrontal cortex (mPFC) are both critical regions for social behaviors. However, how their interactions affect social behavior is not well understood. By viral tracing, optogenetics, chemogenetics, and fiber photometry, we demonstrated that inhibition of vHIP or direct projections from vHIP to mPFC impaired social memory expression. Via rabies retrograde tracing, we found that all three major GABAergic neurons in mPFC received direct inputs from vHIP. Activation of parvalbumin positive (PV+) neurons in mPFC but not somatostatin positive (SST+) neurons can rescue the social memory impairment caused by vHIP inhibition. Furthermore, fiber photometry results demonstrated that social behaviors preferentially recruited PV+ neurons and inhibition of hippocampal neurons disrupted the activity of PV+ neurons during social interactions. These results revealed a new mechanism of how vHIP and mPFC regulate social behavior in complementarity with the existing neural circuitry mechanism.

INTRODUCTION

Normal social behaviors are essential for animals to recognize familiar conspecifics and exhibit normal social interactions (McGraw and Young, 2010; Okuyama et al., 2014). Many brain regions and neural circuits have been involved in social behaviors (McGraw and Young, 2010; Walum and Young, 2018). Specially, recent studies reported that activation of pyramidal neurons in the medial prefrontal cortex (mPFC) that project to subcortical areas or inhibition of pyramidal neurons in the ventral hippocampus (vHIP) that project to nucleus accumbens impaired normal social behavior (Murugan et al., 2017; Okuyama et al., 2016; Brumback et al., 2017). Both human and rodent studies have suggested that GABAergic neurons, especially $PV+_{mPFC}$ (PV+ neurons in mPFC) are essential for normal social behaviors (Hashemi et al., 2017; Kobayashi et al., 2018). The PV+ neuron defects could be observed in postmortem human brain tissue of patients with autism (Hashemi et al., 2017). Furthermore, recent studies using transgenetic tools and mice demonstrated that disrupting the excitatory-inhibitory balance in the mPFC impaired normal social behavior, whereas activation of $PV+_{mPFC}$ could rescue the social behavior defects caused by excitatory-inhibitory imbalance or in autism model mice (Selimbeyoglu et al., 2017; Yizhar et al., 2011). Anatomical studies have suggested that $PV+_{mPFC}$ could be innervated by pyramidal neurons in vHIP (Sun et al., 2019; Gabbott et al., 2002). Specially, in previous studies, we found that the hippocampal pyramidal neurons that target $PV+_{mPFC}$ tend to send their collateral projections to nucleus accumbens (Sun et al., 2019). Since the hippocampus-nucleus accumbens pathway has been suggested to be highly associated to social memory (Okuyama et al., 2016), the hippocampus-$PV+_{mPFC}$ projections may also be involved in the expression of social memory. However, how these interactions affect social behavior is unknown.

To address this issue, we employed viral tracing, optogenetics, chemogenetics, and fiber photometry to investigate the connectivity between vHIP and mPFC. The results showed that pyramidal neurons in vHIP can form direct monosynaptic connectivity with three major types of GABAergic neurons in mPFC. Silencing vHIP or vHIP-mPFC pathway disrupted normal social memory expression but did not affect object recognition memory. By manipulating and monitoring the activity of different GABAergic neurons in mPFC during social interactions with inhibition of vHIP, we identified that $PV+_{mPFC}$ were crucial for social behaviors. These results provide a new mechanism of how vHIP-mPFC circuitry regulates social behavior, which can facilitate the study and treatment of social behavior deficits in neuropsychiatric disorders.

[1]Britton Chance Center for Biomedical Photonics, Wuhan National Laboratory for Optoelectronics-Huazhong University of Science and Technology, Wuhan, Hubei 430074, China

[2]MoE Key Laboratory for Biomedical Photonics, School of Engineering Sciences, Huazhong University of Science and Technology, Wuhan, Hubei 430074, China

[3]HUST-Suzhou Institute for Brainsmatics, JITRI Institute for Brainsmatics, Suzhou 215125, China

[4]These authors contributed equally

[5]Lead Contact

*Correspondence: qluo@mail.hust.edu.cn

https://doi.org/10.1016/j.isci.2020.100894

RESULTS

Three Major Types of GABAergic Neurons in the mPFC Receive Direct Inputs from vHIP

The connections between hippocampus and mPFC have been identified (Parent et al., 2010). To validate the connectivity between hippocampal neurons and different types of neurons in the mPFC, we employed monosynaptic rabies virus (RV) tracing technology (Wall et al., 2010). Briefly, two AAV helper virus that express TVA and rabies glycoprotein were injected into the mPFC of three Cre driver lines that target three major GABAergic neuron types (parvalbumin-expressing, somatostatin-expressing, and vasoactive intestinal peptide-expressing interneurons). The TVA protein provided the receptor for avian sarcoma leucosis virus glycoprotein EnvA-coated RV to enter the Cre-positive neurons, and the rabies glycoprotein provided by AAV can help the rabies glycoprotein gene deficit RV to transfer to the upstream input neurons. After 3 weeks, EnvA-coated RV was injected into the same brain area (Figure 1A). Ten days later, we found massive neurons in the injection site were infected by AAV and RV (Figures 1B and 1C). To validate the specificity of the RV tracing, we performed immunostaining at the injection site. We found that the neurons infected by AAV were restricted to specific neuron types (Figures 1D and 1E). Many upstream brain regions were also infected by RV, including hippocampus (Figure 1F). Specially, we found that three major GABAergic neuron types in the mPFC received inputs from hippocampus, which was consistent with our previous study (Sun et al., 2019). Moreover, we extracted the somata of hippocampal neurons that target different types of GABAergic neurons in mPFC and registered to Allen brain reference atlas (Figure 1G). We found that these input neurons of the mPFC distributed along the proximal-distal axis of the hippocampus and intermingled with each other (Figure 1G). To further confirm the synaptic connectivity between vHIP and different GABAergic neurons in mPFC, we injected AAV2/9-CaMKII-NpHR3.0-YFP into the vHIP and AAV2/9-EF1a-DIO-hCHR2(H134R)-mCherry into the mPFC of different Cre driver lines that target three types of GABAergic neurons (Figures S1A–S1C). Three weeks later, we found that three types of GABAergic neurons in mPFC were heavily innervated by hippocampal axons (Figures S1D–S1F). The somata of GABAergic neurons were surrounded by hippocampal axons (Figures S1D–S1F). These results further indicated that ventral hippocampal neurons can form direct synaptic connectivity with different GABAergic neurons in mPFC.

Inhibition of vHIP or Direct Projection from vHIP to mPFC Impaired Social Memory Expression

To explore the functional impacts of the vHIP-mPFC pathway on social behavior, we used the optogenetics technology. AAV expressing NpHR3.0 under control of CaMKII promoter was injected into the vHIP bilaterally to silence the activity of vHIP (Figures 2A and 2B). Previous studies have shown that silencing vHIP can impair social memory (Okuyama et al., 2016). We assigned the test mice to a similar social discrimination test (SDT) to examine the impairment of social memory after silencing vHIP (20 mW, persistent inhibition) (Figures 2C and 2D). We found that the test mice preferentially interacted with the novel mice rather than littermates under normal circumstances but when vHIP was silenced, this social preference just disappeared (Figures 2E–2G), which was consistent with the previous studies (Okuyama et al., 2016). Furthermore, to examine whether direct projection from vHIP to mPFC was involved in regulating social memory expression, we injected AAV expressing NpHR3.0 under control of CaMKII promoter into the vHIP bilaterally and inhibited the hippocampal fibers in mPFC with 570-nm lasers (20 mW, persistent inhibition). Then we assigned the test mice to SDT to examine the impairment of social memory (Figures 2H–2J). When hippocampal fibers in mPFC were inhibited, the test mice did lose their social preference toward novel mice (Figure 2K). Moreover, inhibition of hippocampal fibers in mPFC did not affect the locomotion of mice (Figures 2L and 2M). Our results suggested that the social memory can be directly transferred from vHIP to mPFC.

Inhibition of vHIP Did Not Affect Object Recognition Memory

Our results have shown that inhibition of vHIP can cause loss of social preference of mice. To test whether inhibition of vHIP can affect the expression of other types of memory, we also inhibited the activity of vHIP with AAV virus and assigned the test mice to novel/familiar object test (Figures 3A and 3B). The novel/familiar object test contained three phases: the acquisition phase, memory consolidation, and the test phase (Figure 3B). In the acquisition phase, test mice were allowed to explore two identical objects for 4 min. Then the test mice were returned to homecage to rest for 10 min for memory consolidation. Ten minutes later, the test mice were assigned to test phase at which the mice were allowed to explore an old object and a novel object for 4 min (Figure 3B). The laser was delivered in the last 3 min of the test phase to examine whether inhibition of vHIP can disrupt the expression of object recognition memory (Figure 3C). During the acquisition phase, the test mice showed no preference toward two identical objects (Figures 3D and 3E). During the test phase, the test

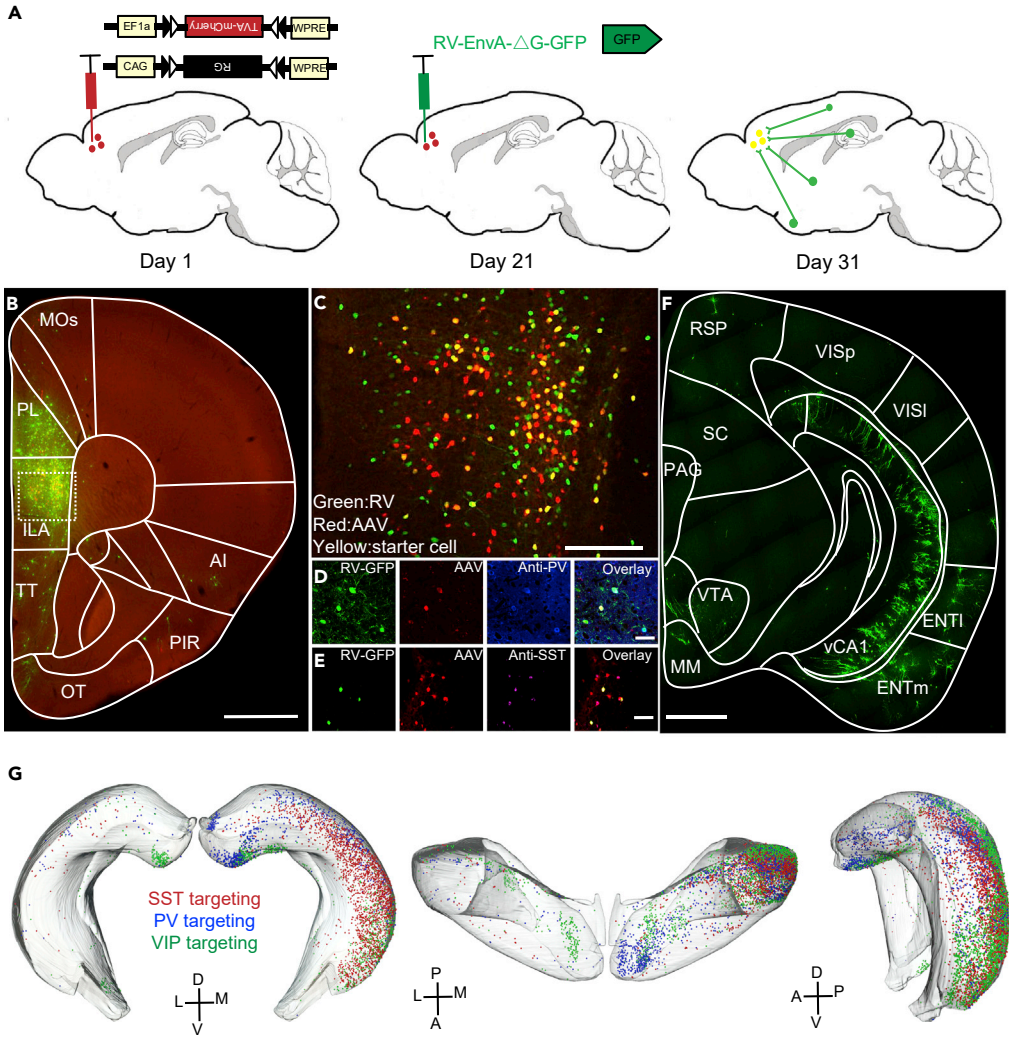

Figure 1. Hippocampal Neurons Innervated Three Major GABAergic Neuron Types in the mPFC

(A) Monosynaptic rabies virus tracing strategy.

(B) Injection site at mPFC.

(C) Enlarged image boxed in (B), showing the AAV, RV, and double labeling neurons. The double labeling neurons were defined as starter cells.

(D and E) Immunostaining against parvalbumin and somatostatin at the injection sites. The TVA-mCherry and EGFP expressed neurons in PV-Cre mice and SST-Cre mice were parvalbumin and somatostatin positive, respectively.

(F) Input neurons from hippocampus.

(G) Distribution of hippocampal neurons targeted three types of GABAergic neuron in the mPFC. Scale bars in (B) and (F) are 1 mm; scale bar in (C) is 200 μm; scale bars in (D) and (E) are 50 μm.

mice showed significant preference toward novel object irrespective of whether the vHIP was silenced or not (Figures 3D–3F), which suggested that silencing vHIP does not affect novel/familiar object recognition memory, which was consistent with previous rat behavioral studies (Mumby, 2001; Albasser et al., 2012). Although the locomotion of the test mice was impaired when vHIP was inhibited (Figure 3D), the object recognition memory of the test mice remained intact (Figure 3F), which suggested that locomotion impairment caused by inhibition of vHIP does not affect the expression of memory.

Activation of PV+$_{mPFC}$ Rescued the Impairment of Social Memory Caused by Inhibition of vHIP

Next, to explore how different types of GABAergic neurons in mPFC regulate the hippocampus-dependent social memory expression, we repeated the social discrimination test with vHIP silenced and

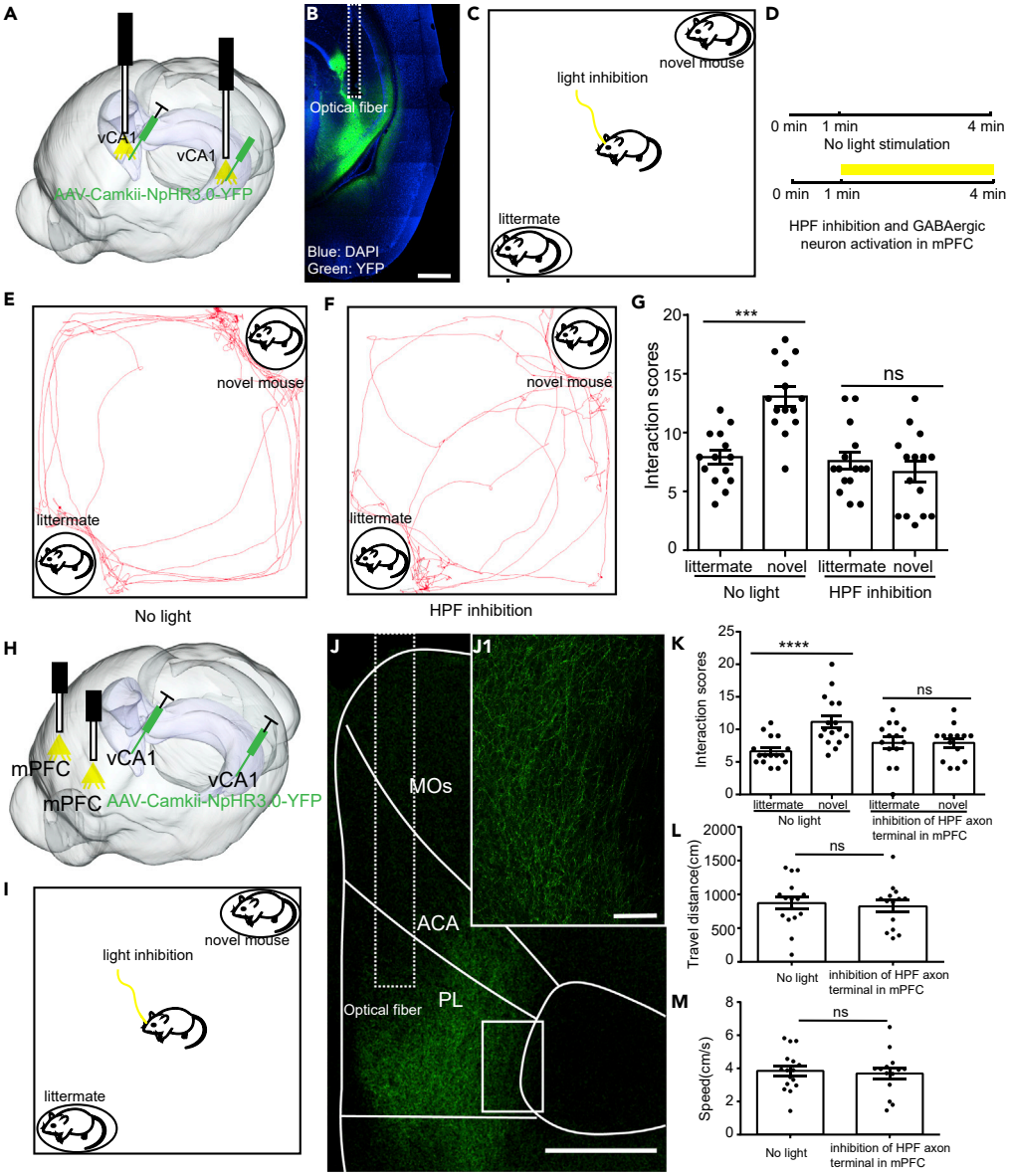

Figure 2. Inhibition of vHIP or the Hippocampal Fibers in mPFC Impaired Social Memory

(A) Schematic of the experimental strategy. AAV-CaMKII-NpHR3.0-YFP was injected into vHIP to silence the activity of vHIP.

(B) Expression of NpHR in vHIP.

(C) Experimental strategy of social discrimination test.

(D) Timeline of social discrimination test.

(E and F) Position tracking from representative mice during social discrimination test with or without light inhibition of vHIP.

(G) Social interaction times with novel mice or littermates with or without light inhibition of vHIP (paired t test, ***$p < 0.001$, control group, n = 14 mice; vHIP inhibition group, n = 15 mice).

(H) Schematic of the experimental strategy. AAV-CaMKII-NpHR3.0-YFP was injected into vHIP and the optical fibers was placed in the mPFC to silence the hippocampal fibers in mPFC.

(I) Experimental strategy of social discrimination test.

(J) The hippocampal axon terminals in mPFC. (J1) Enlarged image boxed in (J).

(K) Inhibition of HIP axon terminals in mPFC affects social memory (control group, n = 16 mice; HIP terminal inhibition group, n = 14 mice. paired t test, ****$p < 0.0001$).

(L and M) Inhibition of HIP axon terminals in mPFC does not affect locomotion (control group, n = 16 mice; HIP terminal inhibition group, n = 14 mice. Unpaired t test). Scale bars in (B) and (J) are 500 μm and in (J1) is 100 μm. ns, no significance. All results are presented as the means ± s.e.m.

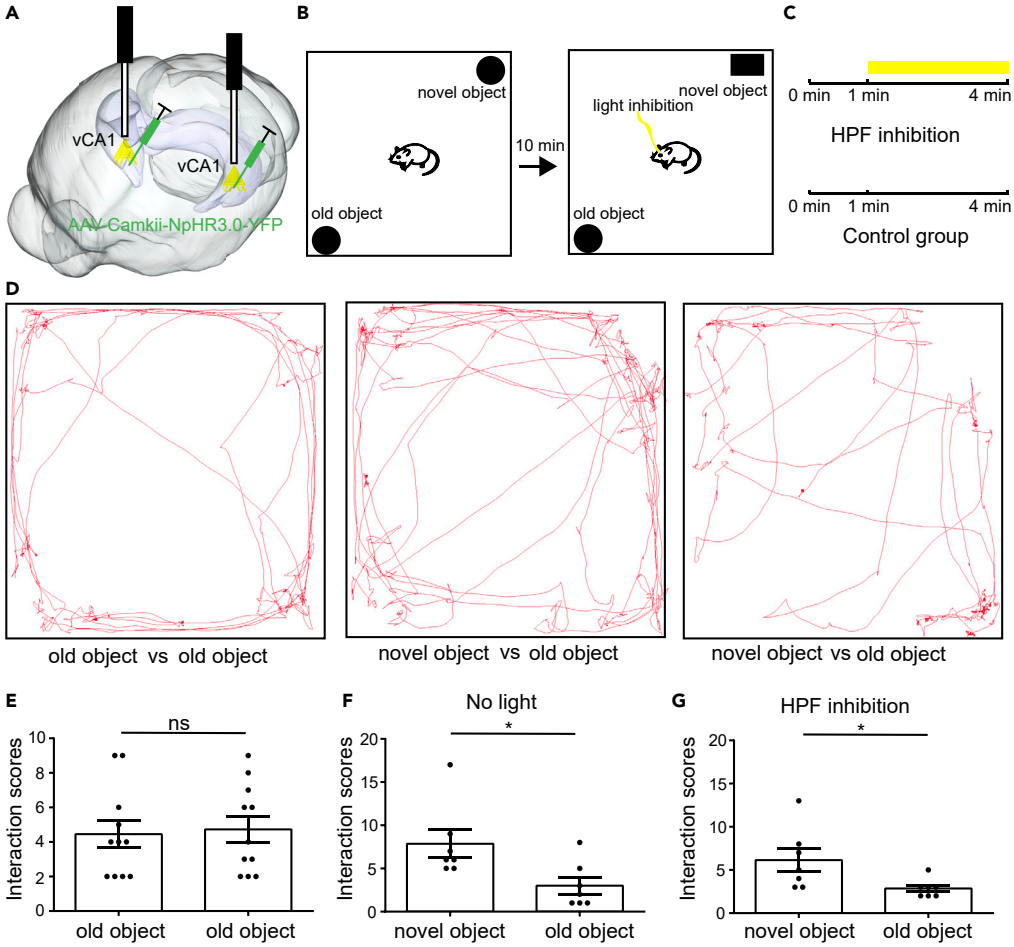

Figure 3. Inhibition of HIP Does Not Affect Object Recognition Memory

(A–C) Experimental procedures of novel/familiar object test with or without inhibition of vHIP.

(D) Position tracking from representative mice during novel/familiar object when mice interact with novel object or familiar object.

(E) Interaction times with familiar objects during test. The mice showed no preference between two identical familiar objects (n = 11).

(F) Interaction times with novel object and familiar object. The mice showed significant preference to novel object (n = 7 mice, paired t test, *p < 0.05).

(G) Interaction times with novel object and familiar object when vHIP was inhibited. The mice showed significant preference to novel object (n = 7, paired t test, *p < 0.05). ns, no significance. All results are presented as the means ± s.e.m.

activated the different types of GABAergic neurons in the mPFC to explore how GABAergic neurons in the mPFC affect social memory (Figures 4A–4C). To validate the specificity of ChR2 expression, we also performed the immunochemical staining against PV, SST, and VIP at the injection site of mPFC. We found that the ChR2 was strictly expressed in specific neuron types (Figures 4D–4F). During social discrimination test, we found that activating $PV+_{mPFC}$ neurons but not $SST+_{mPFC}$ (SST+ neurons in mPFC) can restore the social preference (Figures 4G–4I), which suggested that $PV+_{mPFC}$ are one of the downstream targets of vHIP to convey and express social memory. Interestingly, we found that activation of $VIP+_{mPFC}$ (VIP+ neurons in mPFC) had the opposite effects as the activation of $PV+_{mPFC}$ neurons and caused the loss of social interactions during test (Figure 4I). Inhibition of somata in vHIP also impaired the locomotion of the mice (Figures 4J and 4K), which was consistent with the previous studies that hippocampus is crucial for regulating locomotion (Czurko et al., 1999; Ekstrom et al., 2001; Fuhrmann et al., 2015; Fanselow and Dong, 2010). Surprisingly, we found that activation of $PV+_{mPFC}$ when

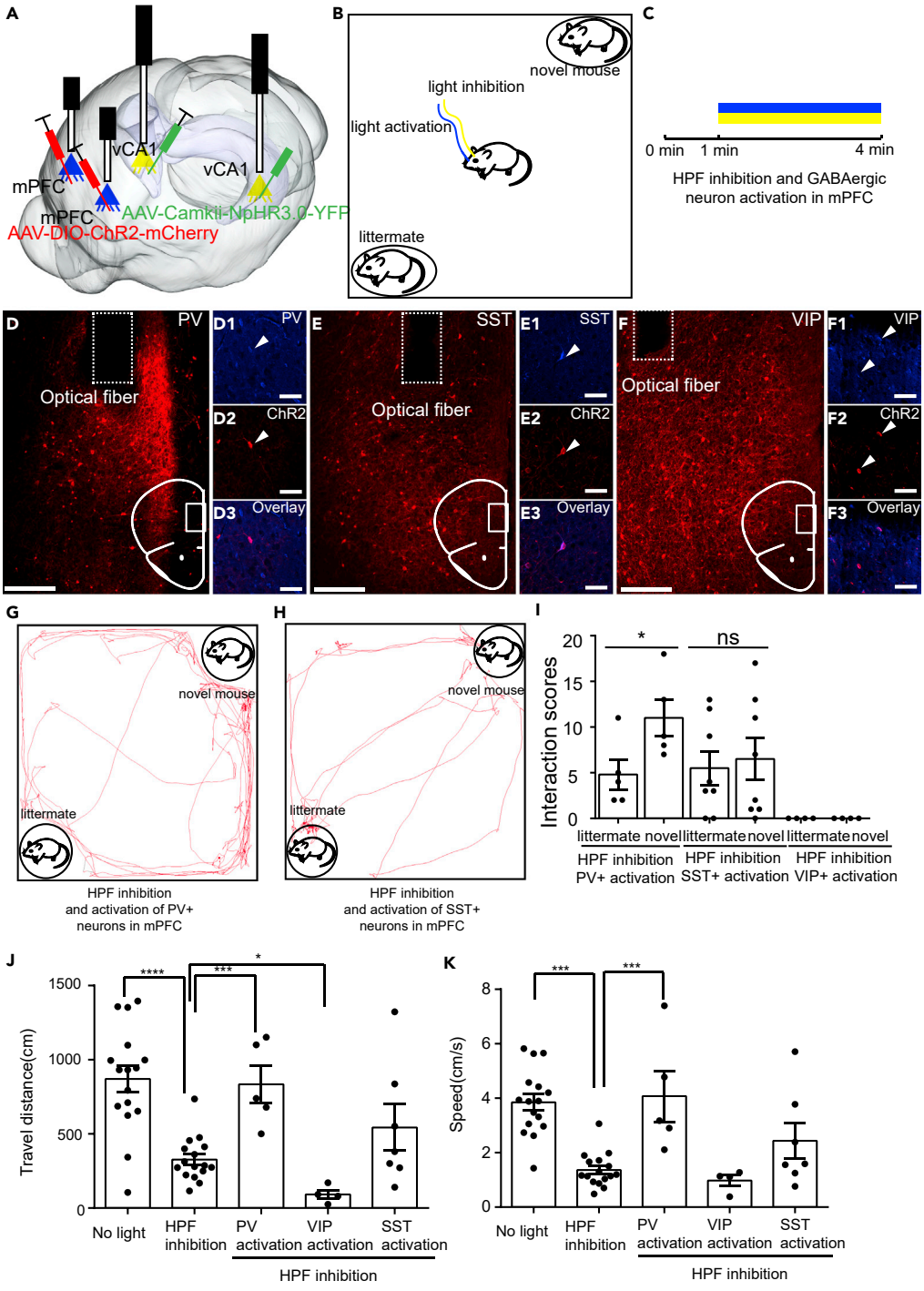

Figure 4. Activation of PV+$_{mPFC}$ Rescued the Social Memory Impairment Caused by Inhibition of vHIP

(A) Schematic of the experimental strategy. AAV-CaMKII-NpHR3.0-YFP was injected into vHIP to silence the activity of vHIP, whereas AAV-DIO-ChR2-mCherry was injected into mPFC to activate the activity of specific types of GABAergic neurons in the mPFC.

(B) Experimental strategy of social discrimination test.

(C) Timeline of social discrimination test.

(D–F) Post hoc lesion analysis of the position of optical fibers for optogenetics and immunostaining to validate the specificity of ChR2 expression.

Figure 4. *Continued*

(G and H) Position tracking from representative mice during social discrimination test with inhibition of vHIP and activation of PV+$_{mPFC}$ or SST+$_{mPFC}$.

(I) Social interaction times with novel mice or littermates with light inhibition of vHIP and light activation of PV+$_{mPFC}$, SST+$_{mPFC}$ neurons, and VIP+$_{mPFC}$ (paired t test, *p < 0.05, PV+, n = 5 mice; SST+, n = 7 mice, VIP+, n = 4 mice).

(J and K) Inhibition of vHIP affects the traveling distance and speed of mice when exploring chambers. Activation of PV+$_{mPFC}$ and VIP+$_{mPFC}$ rescued and worsen the locomotion impairment caused by inhibition of vHIP, respectively (control group, n = 16 mice; vHIP inhibition group, n = 16 mice; PV-Cre mice, n = 5; VIP-Cre mice, n = 4; SST-Cre mice, n = 7. One-way ANOVA followed by Tukey's post hoc tests, *p < 0.05, ***p < 0.001, ****p < 0.0001). Scale bars in (D), (E), (F) are 200 μm and scale bars in (D1)–(D3), (E1)–(E3), and (F1)–(F3) are 50 μm. ns, no significance. All results are presented as the means ± s.e.m.

vHIP was silenced can rescue the locomotion impairment (15 mW, 20 Hz, 15 ms duration) (Figures 4J and 4K), whereas activation of VIP+$_{mPFC}$ (VIP+ neurons in mPFC) can further suppress locomotion (15 mW, 20 Hz, 15-ms duration) (Figure 4J).

Since activation of VIP+$_{mPFC}$ had the opposite effects as the activation of PV+$_{mPFC}$, we wondered whether inhibition of VIP+$_{mPFC}$ can also rescue the social memory impairment caused by inhibition of vHIP. To test this hypothesis, we injected a Cre-dependent AAV virus expressing NpHR3.0 into the mPFC of VIP-Cre mice to silence the activity of VIP+$_{mPFC}$. In the meantime, we employed chemogenetics to silence the activity of vHIP (Figure 5A). Then we assigned the test mice to social discrimination test to examine the social memory expression of the test mice (Figures 5B and 5C). After the test, post hoc lesion analyses were made to examine the NpHR3.0 expression in mPFC and hM4Di expression in vHIP (Figures 5D–5F). During the test, we found that intraperitoneal injection of saline did not affect the social preference of the test mouse toward the novel mouse (Figures 5G and 5J). However, when CNO was injected intraperitoneally to silence the activity of vHIP, the test mice lost their social preference and showed abnormal social memory expression (Figures 5H and 5J). After the injection of CNO, inhibition of VIP+$_{mPFC}$ with 570-nm laser (20 mW, persistent inhibition) restored the social preference of the test mice (Figures 5I and 5J). Inhibition of vHIP with CNO also suppressed the locomotion of the test mice (Figure 5K), which was similar to optogenetics inhibition, whereas inhibition of VIP+$_{mPFC}$ restored the normal locomotion (Figure 5K). These results indicated that the VIP+$_{mPFC}$ performed the opposite role as the PV+$_{mPFC}$ during regulating the expression of social memory.

Previous studies have suggested that CNO can be converted to clozapine and affects the animal behavior (Gomez et al., 2017; MacLaren et al., 2016). To test whether administration of CNO alone can affect social behavior, we delivered CNO or saline to C57BL/6 mice through intraperitoneal injection and assigned the animals to social discrimination test (Figures S2A–S2C). We found that administration of either saline or CNO did not affect the expression of social memory of the test mice (Figures S2D–S2F). These results suggested that administration of CNO alone without hM4Di cannot affect social behavior.

Our results showed that activation of PV+$_{mPFC}$ can rescue abnormal social behavior and locomotion. Given the robust effects on locomotion, it may be difficult to adequately discriminate between pure motor and social impairments resulting from the manipulations. To further prove that activation of PV+$_{mPFC}$ can rescue pure social impairments, we further performed control experiments on PV-Flpo mice. We already showed that inhibition of hippocampal axon terminals in mPFC impaired social memory expression but did not affect locomotion (Figures 2H–2M), so we assumed that inhibition of hippocampal neurons that directly project to mPFC also impaired social memory expression and did not affect locomotion. Therefore, in our control experiment, we injected a Cre-dependent AAV virus expressing hM4Di into the vHIP of PV-Flpo mice (Figure 6A), a retrograde AAV expressing Cre was injected into the mPFC to provide Cre in vHIP for hM4Di expression(Figure 6A). In the meantime, we also injected an flp-dependent AAV virus expressing ChR2 into the mPFC to activate PV+$_{mPFC}$ (Figure 6A). Three weeks after the virus injection, we assigned the mice to social discrimination test (Figures 6B and 6C). After the test, post hoc lesion analyses were made to examine the ChR2 expression in mPFC and hM4Di expression in vHIP (Figures 6D–6F1). Our immunochemical staining results indicated that ChR2 was strictly expressed in PV+$_{mPFC}$ (Figure 6E). In vHIP, we found that hM4Di was expressed in the pyramidal layers of the vHIP (Figures 6F and 6F1), which was consistent with our previous study that hippocampal neurons that directly project to mPFC located in the pyramidal layers (Sun et al., 2019). During behavior test, we found that intraperitoneal injection of saline did not affect the social preference of the test mouse toward the novel mouse (Figures 6G and 6J). However, when CNO was injected intraperitoneally to silence the hippocampal neurons that project to mPFC,

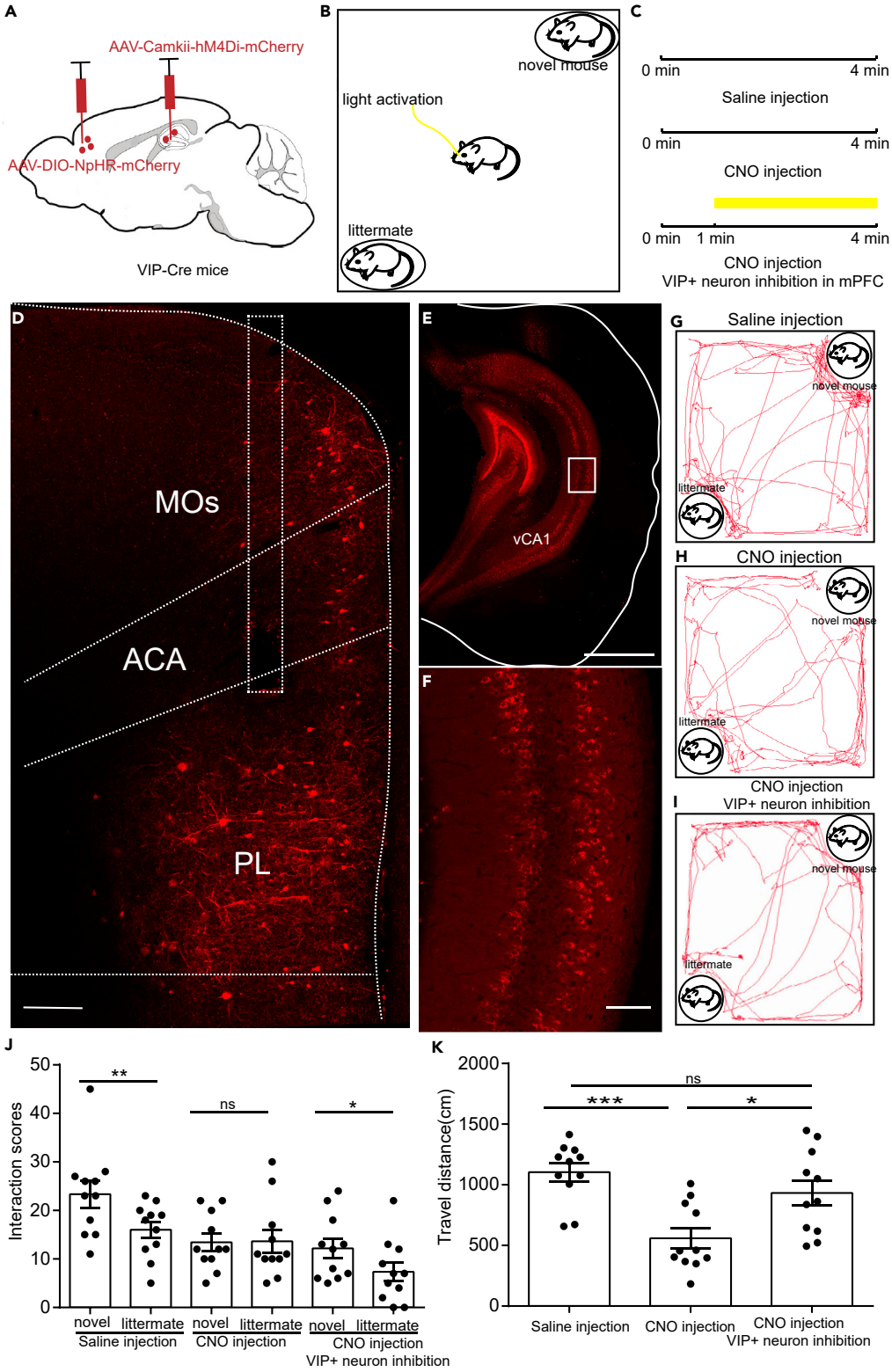

Figure 5. Inhibition of VIP+$_{mPFC}$ Also Rescued the Social Memory Impairment Caused by Inhibition of vHIP

(A) Schematic of the experimental strategy. AAV-CaMKII-hM4Di-mCherry was injected into the vHIP to silence the activity of vHIP, whereas AAV-DIO-NpHR3.0-mCherry was injected into the mPFC to silence the activity of VIP+$_{mPFC}$.

Figure 5. *Continued*

(B) Experimental strategy of social discrimination test.

(C) Timeline of social discrimination test.

(D) The injection site in mPFC.

(E) The injection site in vHIP.

(F) The enlarged image boxed in (E) showing the expression of hM4Di in neurons in vHIP.

(G–I) Position tracking from representative mice during social discrimination test with different experimental conditions.

(J) Social interaction times with novel mice or littermates with different experimental conditions.

(K) The traveling distance of the test mice during social discrimination test with different experimental conditions. Scale bar in (D) is 200 μm. Scale bar in (E) is 1 mm. Scale bar in (F) is 100 μm (for Figure 5J, paired t test, ns, $p > 0.05$, *$p < 0.05$, **$p < 0.01$, n = 11 mice; for Figure 5K, one-way ANOVA followed by Tukey's post hoc tests, *$p < 0.05$, ***$p < 0.001$, ns, $p > 0.05$, n = 11 mice). ns, no significance. All results are presented as the means ± s.e.m.

the test mice lost their social preference and showed abnormal social memory expression (Figures 6H and 6J). After the injection of CNO, activation of PV+$_{mPFC}$ with 470-nm laser (15 mW, 20 Hz, 15-ms duration) restored the social preference of the test mice (Figures 6I and 6J). During all the manipulations, the locomotion of the test mice remained unaltered (Figure 6K). These results suggested that activation of PV+$_{mPFC}$ can rescue pure social memory impairments.

Social Behaviors Preferentially Recruit PV+$_{mPFC}$

Our results have shown that PV+$_{mPFC}$ are one of the downstream targets of vHIP to convey and express social memory. However, how different types of GABAergic neurons in the mPFC participate in social behavior is unclear. Previous studies have shown that PV+$_{mPFC}$ participate in social behavior (Selimbeyoglu et al., 2017). Whether other types of GABAergic neurons in the mPFC participate in social behavior needs to be further investigated. Here we used fiber photometry to explore how different types of GABAergic neurons in the mPFC respond to social behaviors. We injected Cre-dependent AAV expressing GCaMP6s into the mPFC and performed fiber photometry when mice interacted with novel mice or littermates (Figures 7A and 7B). We recorded the calcium signals of SST+$_{mPFC}$ and the social interactions during SDT. Then we aligned the timeline of calcium signals to the timeline of social interactions. We found that the calcium transient duration and the number of interactions were highly aligned (Figure 7C). The number of calcium transient and the number of social interactions were also highly correlated (Figure 7D), which suggested that the activity of SST+$_{mPFC}$ is related to social interactions. We recorded the activity of PV+$_{mPFC}$ neurons and SST+$_{mPFC}$ and found that both PV+ neurons (Figures 7E–7G) and SST+ neurons (Figures 7H–7J) in the mPFC responded to social interaction, whereas the VIP+$_{mPFC}$ did not respond to social interaction (Figures 7K–7M). Although both PV+$_{mPFC}$ neurons and SST+$_{mPFC}$ responded to social interactions, the time window of response is not synchronized. PV+$_{mPFC}$ neurons responded to social interactions after the social interactions happened, whereas SST+$_{mPFC}$ neurons responded to social interactions before the social interactions happened (Figures 7N and 7O). When mice interacted with novel mice or littermates, the response of PV+$_{mPFC}$ neurons or SST+$_{mPFC}$ neurons showed no significant difference (Figures 7P and 7Q). However, the response of PV+$_{mPFC}$ neurons is stronger than that of SST+$_{mPFC}$ neurons (Figure 7R, **unpaired t test, $p < 0.01$**), which indicates that social behaviors preferentially recruit PV+$_{mPFC}$.

Inhibition of vHIP Disrupts the Activity of PV+$_{mPFC}$ but Not SST+$_{mPFC}$ during Social Interactions

Both previous studies and our results have shown that inhibition of vHIP impaired normal social behavior (Okuyama et al., 2016), whereas the GABAergic neurons in the mPFC are also crucial for social behaviors. However, how inhibition of vHIP affects the activity of GABAergic neurons in the mPFC is unclear. To examine how inhibition of vHIP affects the activity of GABAergic neurons in the mPFC, here we injected AAV expressing NpHR3.0 under control of CaMKII promoter to silence vHIP and Cre-dependent AAV expressing GCaMP6s into the mPFC to monitor the activity of GABAergic neurons in the mPFC during inhibition of vHIP (Figure 8A). We assigned the test mice to SDT and monitored the activity of GABAergic neurons in mPFC with vHIP silenced (Figures 8B and 8C). We found that, when vHIP was silenced, the response of PV+$_{mPFC}$ to littermates was decreased compared with that to novel mice (Figures 8D–8F), whereas the activity of SST+$_{mPFC}$ was unaltered (Figures 8G–8I). These results suggested that inhibition of vHIP disrupts the activity of PV+$_{mPFC}$ but not SST+$_{mPFC}$ during social interactions.

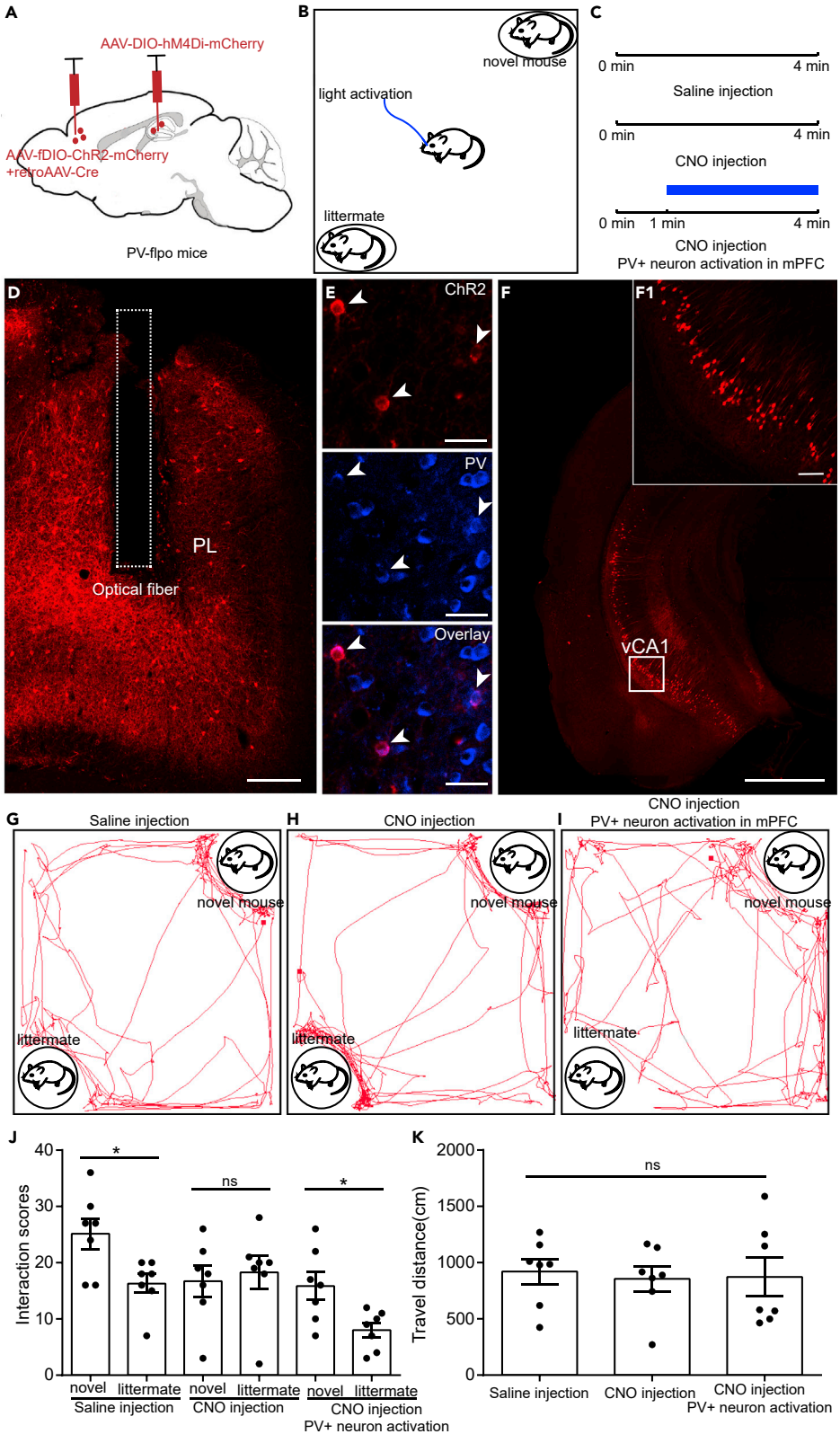
A
AAV-DIO-hM4Di-mCherry
AAV-fDIO-ChR2-mCherry
+retroAAV-Cre
PV-flpo mice
B
novel mouse
light activation
littermate
C
0 min
4 min
Saline injection
0 min
4 min
CNO injection
0 min
1 min
4 min
CNO injection
PV+ neuron activation in mPFC
D
PL
Optical fiber
E
ChR2
PV
Overlay
F
F1
vCA1
G
Saline injection
novel mouse
littermate
H
CNO injection
novel mouse
littermate
I
CNO injection
PV+ neuron activation in mPFC
novel mouse
littermate
J
Interaction scores
40
30
20
10
0
*
ns
*
novel
littermate
novel
littermate
novel
littermate
Saline injection
CNO injection
CNO injection
PV+ neuron activation
K
Travel distance(cm)
2000
1500
1000
500
0
ns
Saline injection
CNO injection
CNO injection
PV+ neuron activation

Figure 6. Activation of PV+$_{mPFC}$ Rescued the Social Memory Impairment Caused by Ventral Hippocampal-mPFC Pathway Inhibition

(A) Schematic of the experimental strategy. AAV-DIO-hM4Di-mCherry was injected into the vHIP of PV-flpo mice to silence the ventral hippocampal-mPFC pathway. A viral mixture containing AAV-fDIO-ChR2-mCherry and retroAAV-Cre was injected into the mPFC of PV-flpo mice to activate PV+$_{mPFC}$ and to provide Cre for AAV-DIO-hM4Di-mCherry expression in vHIP.

(B) Experimental strategy of social discrimination test.

(C) Timeline of social discrimination test.

(D) The injection site in mPFC.

(E) Immunostaining against PV to prove the specificity of ChR2 expression in mPFC.

(F) The injection site in vHIP. (F1) The enlarged image boxed in (F) showing the expression of hM4Di in neurons in vHIP.

(G–I) Position tracking from representative mice during social discrimination test with different experimental conditions.

(J) Social interaction times with novel mice or littermates with different experimental conditions.

(K) The traveling distance of the test mice during social discrimination test with different experimental conditions. Scale bar in (D) is 200 μm. Scale bar in (E) is 30 μm. Scale bar in (F) is 1 mm. Scale bar in (F1) is 100 μm (for Figure 6J, paired t test, ns, $p > 0.05$, *$p < 0.05$, $n = 7$ mice; for Figure 6K, one-way ANOVA followed by Tukey's post hoc tests, ns, $p > 0.05$, $n = 7$ mice). ns, no significance. All results are presented as the means ± s.e.m.

DISCUSSION

In the present study, we discovered that vHIP can innervate three major types of GABAergic neurons in the mPFC (Figure 1) and convey social memory to PV+$_{mPFC}$ neurons. Inhibition of vHIP or direct hippocampal projections to mPFC impaired social memory but not object recognition memory (Figures 2 and 3). Activation of PV+$_{mPFC}$ can rescue the social memory and locomotion impairment caused by inhibition of vHIP (Figures 4 and 6). Both PV+$_{mPFC}$ neurons and SST+$_{mPFC}$ responded to social interactions, and social behaviors preferentially recruit PV+$_{mPFC}$ neurons (Figure 7). Moreover, inhibition of vHIP disrupted the activity of PV+$_{mPFC}$ neurons but not SST+$_{mPFC}$ (Figure 8). Based on our results, we came up with a new circuitry mechanism of how vHIP-mPFC interaction affects social memory and locomotion.

Possible Circuitry Mechanisms of How vHIP-mPFC Interaction Affects Social Memory and Locomotion

Previous studies have shown that pyramidal neurons in mPFC that target multiple subcortical areas such as ACB, MD, and PAG are critical for social behavior (Brumback et al., 2017; Murugan et al., 2017; Franklin et al., 2017). Activation of pyramidal neurons in the mPFC that project to subcortical areas impaired normal social behavior (Brumback et al., 2017; Murugan et al., 2017), whereas another study reported that vHIP can project to mPFC and drive feedforward inhibition onto pyramidal neurons via PV+$_{mPFC}$ (Marek et al., 2018). Loss of hippocampal inputs to mPFC will lead to evaluated excitability of pyramidal neurons and impaired contextual fear memory recall. Activation of PV+$_{mPFC}$ can restore normal contextual fear memory relapse. It is very likely that the vHIP projections to pyramidal neurons in mPFC was dominated by feedforward inhibition driven by PV+$_{mPFC}$ (Marek et al., 2018). The PV+$_{mPFC}$ can be activated by vHIP to inhibit the pyramidal neurons in mPFC that project to subcortical areas such as ACB, MD, and PAG to maintain normal social behavior, whereas inhibition of vHIP retracted the excitatory driving force of PV+$_{mPFC}$ and may lead to evaluated cellular E/I imbalance within the mouse medial prefrontal cortex, which can lead to profound impairment of mPFC functions (Yizhar et al., 2011). Pyramidal neurons in mPFC also received monosynaptic inputs from vHIP (DeNardo et al., 2015; Phillips et al., 2019). A recent study reported that, in a mouse model of autism with severe social behavior impairment, the vHIP formed stronger synaptic connections with layer V pyramidal neurons in mPFC and led to an elevated activity of pyramidal neurons in mPFC (Phillips et al., 2019). Inhibition of pyramidal neurons in mPFC of mouse model of autism can restore the normal social behavior. These findings are also consistent with the hypothesis that evaluated cellular E/I imbalance within mPFC can lead to social behavior impairment.

On the other hand, functional studies have suggested that the maintenance of normal functions of hippocampus-mPFC circuitry rely on the synchronization firing between two brain areas (Eichenbaum, 2017; Place et al., 2016). Inhibition of vHIP may disrupt the synchronization firing between hippocampus and mPFC, which led to abnormal behaviors, whereas activation of PV+$_{mPFC}$ can inhibit the activity of mPFC, which may synchronize the activity of hippocampus and mPFC again and rescues the functional impairment. Previous functional study on human has shown that hippocampus and

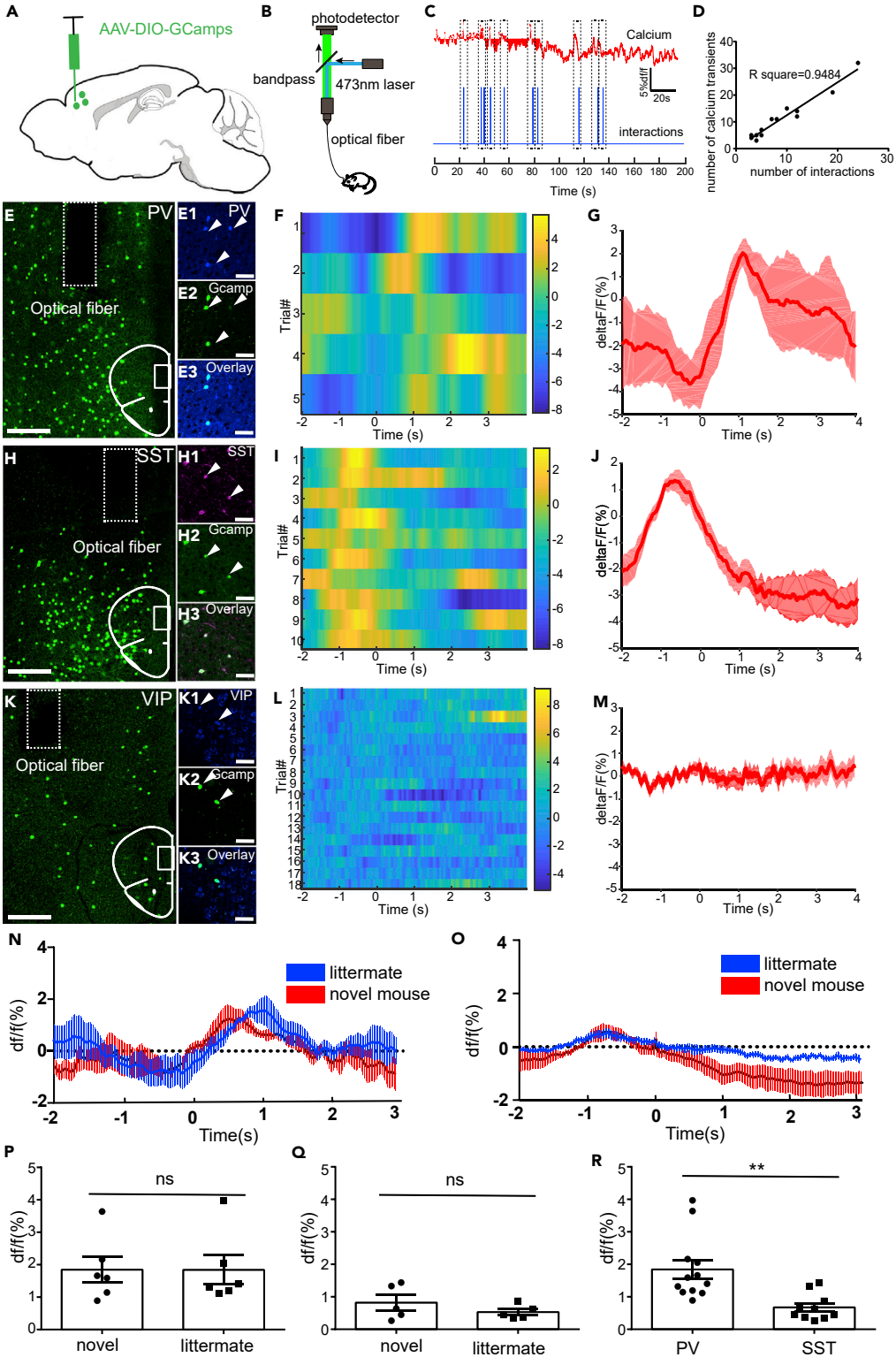

Figure 7. PV+$_{mPFC}$ Neurons and SST+$_{mPFC}$ Are Both Activated during Social Interactions

(A and B) Fiber photometry recordings were performed on different types of GABAergic neurons in the mPFC during social interactions with novel mice or littermates.

Figure 7. *Continued*

(C) An example results of fiber photometry recordings during 200 s showed the alignment between calcium signals and social interactions.

(D) The correlation between numbers of social interactions and numbers of calcium transients.

(E–E3) Post hoc lesion analysis of the position of optical fibers for fiber photometry and immunostaining to validate the specificity of GCaMP expression in PV+ neurons.

(F) Heatmap of Ca^{2+} transients of $PV+_{mPFC}$ during social interactions.

(G) Average plots show that social interactions activated $PV+_{mPFC}$.

(H–H3) Post hoc lesion analysis of the position of optical fibers for photometry and immunostaining to validate the specificity of GCaMP expression in SST+ neurons.

(I) Heatmap of Ca^{2+} transients of $SST+_{mPFC}$ during social interactions.

(J) Average plots show that social interactions activated $SST+_{mPFC}$.

(K–K3) Post hoc lesion analysis of the position of optical fibers for photometry and immunostaining to validate the specificity of GCaMP expression in VIP+ neurons.

(L) Heatmap of Ca^{2+} transients of $VIP+_{mPFC}$ during social interactions.

(M) Average plots show that $VIP+_{mPFC}$ did not respond to social interactions. Scale bars in (E), (H), and (K) are 200 μm; scale bars in (E1)–(E3), (H1)–(H3), and (K1)–(K3) are 50 μm.

(N) Fiber photometry recordings were performed on $PV+_{mPFC}$ during social interactions with novel mice or littermates (n = 6 mice).

(O) Fiber photometry recordings were performed on $SST+_{mPFC}$ during social interactions with novel mice or littermates (n = 5 mice).

(P and Q) Quantification of peak DF/F signals recorded from $PV+_{mPFC}$ and $SST+_{mPFC}$ during social interactions with novel mice or littermates.

(R) Quantification of peak DF/F signals recorded from $PV+_{mPFC}$ neurons and $SST+_{mPFC}$ neurons during social interactions with novel mice (unpaired t test, $^{**}p < 0.01$). ns, no significance. All results are presented as the means ± s.e.m.

neocortical inhibition are essential for memory separation (Koolschijn et al., 2019), whereas our study further demonstrated that activation of $PV+_{mPFC}$ by hippocampus is critical for expression of social memory.

Our results also showed that inhibition of vHIP affected locomotion but inhibition of hippocampal fibers in the mPFC did not affect locomotion (Figure 2). These results suggested social memory and locomotion information flow from vHIP to mPFC through separated pathways, whereas these information was finally convergent to $PV+_{mPFC}$. The VIP+ neurons are known to drive disinhibition in the cortex (Pi et al., 2013). In our results, we found that activation of $VIP+_{mPFC}$ can further suppress social interactions and locomotion during inhibition of vHIP (Figure 2), whereas inhibition of $VIP+_{mPFC}$ can restore social memory expression, which suggested that activation of $VIP+_{mPFC}$ may cause more inhibition onto $PV+_{mPFC}$ to worsen the normal social interactions and locomotion. Previous studies have shown that the glutamatergic inputs from medial septum to hippocampus are essential for regulating locomotion (Fanselow and Dong, 2010; Fuhrmann et al., 2015). Several downstream areas of hippocampus such as lateral and medial septum, retrosplenial cortex, and entorhinal cortex are involved in locomotion regulation (Fanselow and Dong, 2010). These areas can send direct monosynaptic inputs to $PV+_{mPFC}$(Sun et al., 2019). Therefore, these brain areas can be the candidate brain areas that carry the locomotion information from hippocampus to $PV+_{mPFC}$.

The Roles of $PV+_{mPFC}$ Neurons and $SST+_{mPFC}$ during Social Interactions

Our results suggested that both $PV+_{mPFC}$ neurons and $SST+_{mPFC}$ responded to social behaviors (Figure 7); however, the response of $PV+_{mPFC}$ neurons are stronger than that of $SST+_{mPFC}$. Specially, we found that the time window of response between PV+ neurons and SST+ neurons is not synchronized (Figure 7). A previous study using reward foraging task also showed that $PV+_{mPFC}$ neurons and $SST+_{mPFC}$ responded differently to reward signals (Kvitsiani et al., 2013). $PV+_{mPFC}$ neurons responded strongly during reward zone exit, whereas $SST+_{mPFC}$ neurons responded strongly during reward zone entry. Social interactions are often considered as mild reward. Thus, our results were consistent with the previous study, which suggested that $SST+_{mPFC}$ neurons and $PV+_{mPFC}$ responded strongly before and after reward, respectively.

Our optogenetics results showed that activation of $PV+_{mPFC}$ but not $SST+_{mPFC}$ can rescue the social memory expression impairment caused by inhibition of hippocampus. Calcium dynamics of these two

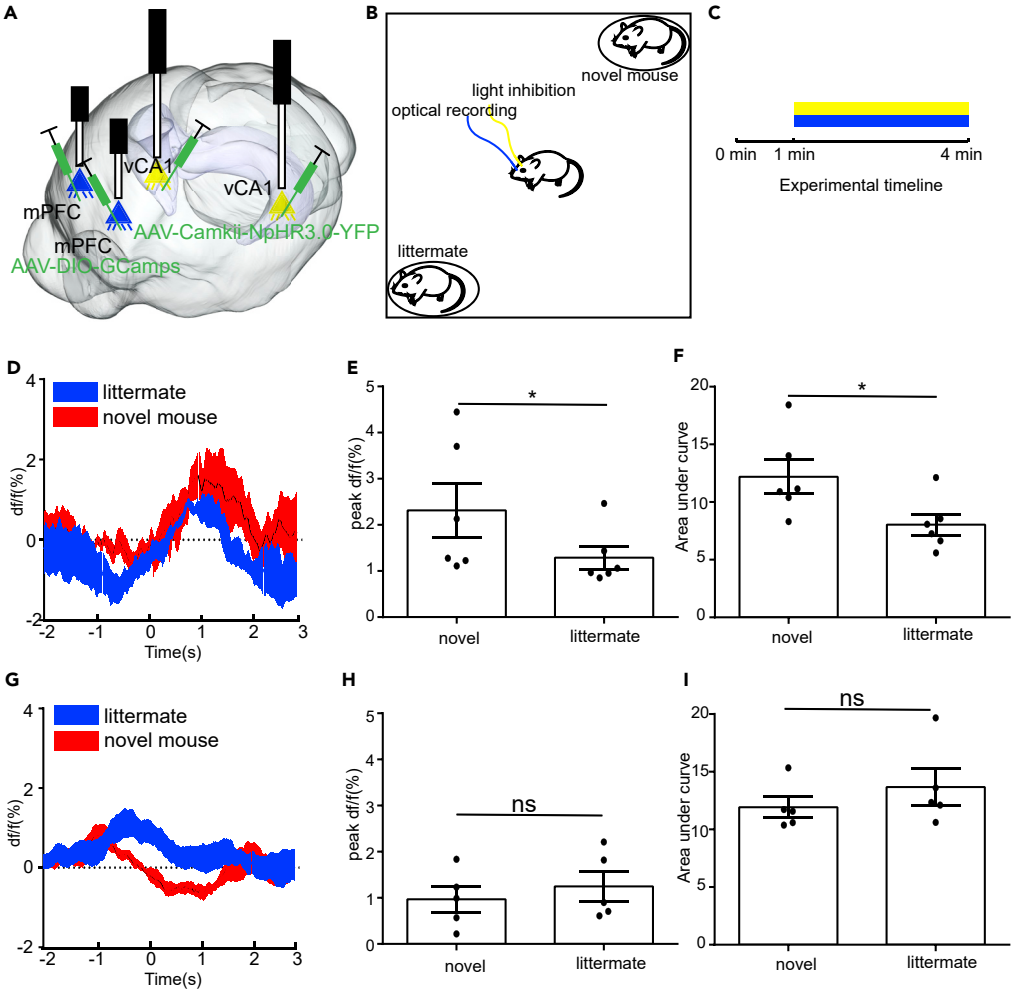

Figure 8. Inhibition of vHIP Disrupts the Activity of PV+$_{mPFC}$ during Social Interactions

(A) Schematic of the experimental strategy. AAV-CaMKII-NpHR3.0-YFP was injected into vHIP to silence the activity of vHIP, whereas AAV-DIO-GCaMP6s was injected into mPFC to monitor the activity of specific types of GABAergic neurons in the mPFC.

(B) Experimental strategy of social discrimination test.

(C) Timeline of social discrimination test.

(D) Fiber photometry recordings were performed on PV+$_{mPFC}$ during social interactions with novel mice or littermates with inhibition of vHIP (n = 6 mice).

(E) Quantification of peak DF/F signals recorded from PV+$_{mPFC}$ during social interactions with novel mice or littermates (paired t test, *p < 0.05).

(F) Quantification of the area under curve of calcium signals recorded from PV+$_{mPFC}$ during social interactions with novel mice or littermates (paired t test, *p < 0.05).

(G) Fiber photometry recordings were performed on SST+$_{mPFC}$ during social interactions with novel mice or littermates with inhibition of vHIP (paired t test, n = 5 mice).

(H) Quantification of peak DF/F signals recorded from SST+$_{mPFC}$ during social interactions with novel mice or littermates.

(I) Quantification of the area under curve of calcium signals recorded from SST+$_{mPFC}$ during social interactions with novel mice or littermates (paired t test, n = 5 mice). ns, no significance. All results are presented as the means ± s.e.m.

types of neurons during social interactions also showed that social interactions preferentially recruited PV+$_{mPFC}$. Activation of VIP+$_{mPFC}$ during SDT with vHIP silenced have the opposite effects as the PV+$_{mPFC}$ neuron activation and can cause the loss of social interactions during the test. Fiber photometry results also showed that during social interaction, VIP+$_{mPFC}$ showed little response. These results showed that

PV+$_{mPFC}$ are more essential for social behaviors, whereas the SST+$_{mPFC}$ neurons and VIP+$_{mPFC}$ may play more critical roles in other functions, such as spatial working memory (Abbas et al., 2018) and anxiety (Lee et al., 2019).

Several studies have suggested that PV+$_{mPFC}$ are critical for social behavior (Ferguson and Gao, 2018; Selimbeyoglu et al., 2017; Yizhar et al., 2011). Our results also indicated that PV+$_{mPFC}$ are essential for hippocampus-dependent social memory expression. However, our results along with other studies suggested that PV+$_{mPFC}$ do not differentially respond to the novel or familiar mouse (Selimbeyoglu et al., 2017), which implied that PV+$_{mPFC}$ are not social discriminators but are critical for modulation of social discriminators. In previous studies, PV+$_{mPFC}$ have been shown to be critical for social behavior in pathophysiological conditions (Ferguson and Gao, 2018; Selimbeyoglu et al., 2017; Yizhar et al., 2011). However, under normal conditions, optogenetical manipulation of PV+$_{mPFC}$ did not affect social behaviors (Yizhar et al., 2011), which further implied that PV+$_{mPFC}$ are not social discriminators but are critical for modulation of social discriminators. Considering that PV+$_{mPFC}$ are critical for modulating the excitability of pyramidal neurons to maintain the normal social functions of mPFC (Marek et al., 2018; Ferguson and Gao, 2018), it is likely that the subgroups of pyramidal neurons in mPFC played the role of social discriminator.

Inhibition of vHIP and Model of Autism

In our results, we found that inhibition of vHIP can disrupt the normal activity of PV+$_{mPFC}$ and lead to a decreased response to littermates (Figure 8). Interestingly, this phenomenon was also observed in a mouse model of autism with abnormal social behavior (Selimbeyoglu et al., 2017). A recent study also found that, in a mouse model of autism, the hippocampus-mPFC pathway was altered and led to the abnormal social behaviors of mice (Phillips et al., 2019). These results along with our findings suggested that the vHIP-mPFC circuitry and PV+$_{mPFC}$ can become new treatment targets for autism like neuropsychiatric disorders.

Limitations of the Study

In the present study, we used the NpHR to inhibit the vHIP and ChR2 to activate the specific GABAergic neurons in mPFC in the same brain. It is likely that optogenetic stimulation of the mPFC with a 470-nm laser will simultaneously activate hippocampal fibers in mPFC that express NpHR, although it is likely that the 470-nm activation of the cell bodies of the interneurons would override this effect. Using chemogenetic viral tools in combination with optogenetic viral tools may overcome this limitation.

On the other hand, owing to the limitation of current techniques, it remained unclear whether the hippocampal neurons that target different types of neurons in mPFC are the same neurons or different neurons. For example, the hippocampal neurons that target PV+$_{mPFC}$ may also target other interneuron subtypes or even pyramidal neurons in mPFC. Therefore, when we manipulated the hippocampal neurons, the activity of multiple types of neurons in mPFC may be affected, which made the effects of manipulations in the present study not intuitive. In future studies, new techniques and tools are required to further deconstruct the hippocampal-mPFC pathway. If we can isolate and target the hippocampal neurons that project to the single specific types of neurons in mPFC alone, we can study the functions of hippocampal-mPFC pathway in a more transparent manner.

In general, we explored the functional contributions of hippocampus-mPFC circuitry on social behaviors. Our results suggested that vHIP can transfer social memory to PV+$_{mPFC}$. Activation of PV+$_{mPFC}$ can rescue the social memory impairment caused by inhibition of vHIP. Inhibition of hippocampus also disrupted the normal activity of PV+$_{mPFC}$. Taken together, our results revealed a new mechanism of how vHIP and mPFC regulate social behavior and provided a new potential treatment target for neuropsychiatric disorders.

METHODS

All methods can be found in the accompanying Transparent Methods supplemental file.

SUPPLEMENTAL INFORMATION

Supplemental Information can be found online at https://doi.org/10.1016/j.isci.2020.100894.

ACKNOWLEDGMENTS

We thank Miao Ren, Jing Yuan, and Xueyan Jia for help with experiments and data analysis. We thank the Optical Bioimaging Core Facility of HUST for support with data acquisition. This work was financially supported by National Natural Science Foundation of China (NSFC, Nos. 61721092, 61890953, 31871088) and the Director Fund of Wuhan National Laboratory for Optoelectronics.

AUTHOR CONTRIBUTIONS

Q.L., H.G., and X.L. conceived and designed the study. Q.S., X.L., and J.Z. performed the experiments and analyzed the data. Z.D. performed the whole-brain data acquisition. A.L. performed the whole-brain data processing. Q.L., H.G., X.L., and Q.S. wrote the paper.

DECLARATION OF INTERESTS

The authors declare that the research was conducted in the absence of any commercial or financial relationships that could be construed as a potential conflict of interest.

Received: March 23, 2019
Revised: September 23, 2019
Accepted: February 4, 2020
Published: March 27, 2020

REFERENCES

Abbas, A.I., Sundiang, M.J.M., Henoch, B., Morton, M.P., Bolkan, S.S., Park, A.J., Harris, A.Z., Kellendonk, C., and Gordon, J.A. (2018). Somatostatin interneurons facilitate hippocampal-prefrontal synchrony and prefrontal spatial encoding. Neuron *100*, 926–939.e3.

Albasser, M.M., Amin, E., Lin, T.C.E., Iordanova, M.D., and Aggleton, J.P. (2012). Evidence that the rat Hippocampus has contrasting roles in object recognition memory and object recency memory. Behav. Neurosci. *126*, 659–669.

Brumback, A.C., Ellwood, I.T., Kjaerby, C., Iafrati, J., Robinson, S., Lee, A.T., Patel, T., Nagaraj, S., Davatolhagh, F., and Sohal, V.S. (2017). Identifying specific prefrontal neurons that contribute to autism-associated abnormalities in physiology and social behavior. Mol. Psychiatry *23*, 2078–2089.

Czurko, A., Hirase, H., Csicsvari, J., and Buzsaki, G. (1999). Sustained activation of hippocampal pyramidal cells by 'space clamping' in a running wheel. Eur. J. Neurosci. *11*, 344–352.

DeNardo, L.A., Berns, D.S., DeLoach, K., and Luo, L. (2015). Connectivity of mouse somatosensory and prefrontal cortex examined with trans-synaptic tracing. Nat. Neurosci. *18*, 1687–1697.

Eichenbaum, H. (2017). Prefrontal-hippocampal interactions in episodic memory. Nat. Rev. Neurosci. *18*, 547–558.

Ekstrom, A.D., Meltzer, J., McNaughton, B.L., and Barnes, C.A. (2001). NMDA receptor antagonism blocks experience-dependent expansion of hippocampal "place fields". Neuron *31*, 631–638.

Fanselow, M.S., and Dong, H.W. (2010). Are the dorsal and ventral hippocampus functionally distinct structures? Neuron *65*, 7–19.

Ferguson, B.R., and Gao, W.J. (2018). Thalamic control of cognition and social behavior via regulation of gamma-aminobutyric acidergic signaling and excitation/inhibition balance in the medial prefrontal cortex. Biol. Psychiatry *83*, 657–669.

Franklin, T.B., Silva, B.A., Perova, Z., Marrone, L., Masferrer, M.E., Zhan, Y., Kaplan, A., Greetham, L., Verrechia, V., Halman, A., et al. (2017). Prefrontal cortical control of a brainstem social behavior circuit. Nat. Neurosci. *20*, 260–270.

Fuhrmann, F., Justus, D., Sosulina, L., Kaneko, H., Beutel, T., Friedrichs, D., Schoch, S., Schwarz, M.K., Fuhrmann, M., and Remy, S. (2015). Locomotion, Theta oscillations, and the speed-correlated firing of hippocampal neurons are controlled by a medial septal glutamatergic circuit. Neuron *86*, 1253–1264.

Gabbott, P., Headlam, A., and Busby, S. (2002). Morphological evidence that CA1 hippocampal afferents monosynaptically innervate PV-containing neurons and NADPH-diaphorase reactive cells in the medial prefrontal cortex (Areas 25/32) of the rat. Brain Res. *946*, 314–322.

Gomez, J.L., Bonaventura, J., Lesniak, W., Mathews, W.B., Sysa-Shah, P., Rodriguez, L.A., Ellis, R.J., Richie, C.T., Harvey, B.K., Dannals, R.F., et al. (2017). Chemogenetics revealed: DREADD occupancy and activation via converted clozapine. Science *357*, 503–507.

Hashemi, E., Ariza, J., Rogers, H., Noctor, S.C., and Martinez-Cerdeno, V. (2017). The number of parvalbumin-expressing interneurons is decreased in the medial prefrontal cortex in autism. Cereb. Cortex *27*, 1931–1943.

Kobayashi, M., Hayashi, Y., Fujimoto, Y., and Matsuoka, I. (2018). Decreased parvalbumin and somatostatin neurons in medial prefrontal cortex in BRINP1-KO mice. Neurosci. Lett. *683*, 82–88.

Koolschijn, R.S., Emir, U.E., Pantelides, A.C., Nili, H., Behrens, T.E.J., and Barron, H.C. (2019). The Hippocampus and neocortical inhibitory engrams protect against memory interference. Neuron *101*, 528–539.

Kvitsiani, D., Ranade, S., Hangya, B., Taniguchi, H., Huang, J.Z., and Kepecs, A. (2013). Distinct behavioural and network correlates of two interneuron types in prefrontal cortex. Nature *498*, 363–366.

Lee, A.T., Cunniff, M.M., See, J.Z., Wilke, S.A., Luongo, F.J., Ellwood, I.T., Ponnavolu, S., and Sohal, V.S. (2019). VIP interneurons contribute to avoidance behavior by regulating information flow across hippocampal-prefrontal networks. Neuron *102*, 1223–1234.e4.

MacLaren, D.A., Browne, R.W., Shaw, J.K., Krishnan Radhakrishnan, S., Khare, P., Espana, R.A., and Clark, S.D. (2016). Clozapine N-oxide administration produces behavioral effects in long-evans rats: implications for designing DREADD experiments. eNeuro *3*, 1–14, e0219–16.2016.

Marek, R., Jin, J., Goode, T.D., Giustino, T.F., Wang, Q., Acca, G.M., Holehonnur, R., Ploski, J.E., Fitzgerald, P.J., Lynagh, T., et al. (2018). Hippocampus-driven feed-forward inhibition of the prefrontal cortex mediates relapse of extinguished fear. Nat. Neurosci. *21*, 384–392.

McGraw, L.A., and Young, L.J. (2010). The prairie vole: an emerging model organism for understanding the social brain. Trends Neurosci. *33*, 103–109.

Mumby, D.G. (2001). Perspectives on object-recognition memory following hippocampal damage: lessons from studies in rats. Behav. Brain Res. *127*, 159–181.

Murugan, M., Jang, H.J., Park, M., Miller, E.M., Cox, J., Taliaferro, J.P., Parker, N.F., Bhave, V., Hur, H., Liang, Y., et al. (2017). Combined social and spatial coding in a descending projection from the prefrontal cortex. Cell *171*, 1663–1677.e16.

Okuyama, T., Kitamura, T., Roy, D.S., Itohara, S., and Tonegawa, S. (2016). Ventral CA1 neurons store social memory. Science *353*, 1536–1541.

Okuyama, T., Yokoi, S., Abe, H., Isoe, Y., Suehiro, Y., Imada, H., Tanaka, M., Kawasaki, T., Yuba, S., Taniguchi, Y., et al. (2014). A neural mechanism underlying mating preferences for familiar individuals in medaka fish. Science *343*, 91–94.

Parent, M.A., Wang, L., Su, J., Netoff, T., and Yuan, L.L. (2010). Identification of the hippocampal input to medial prefrontal cortex in vitro. Cereb. Cortex *20*, 393–403.

Phillips, M.L., Robinson, H.A., and Pozzo-Miller, L. (2019). Ventral hippocampal projections to the medial prefrontal cortex regulate social memory. Elife *8*, e44182.

Pi, H.J., Hangya, B., Kvitsiani, D., Sanders, J.I., Huang, Z.J., and Kepecs, A. (2013). Cortical interneurons that specialize in disinhibitory control. Nature *503*, 521–524.

Place, R., Farovik, A., Brockmann, M., and Eichenbaum, H. (2016). Bidirectional prefrontal-hippocampal interactions support context-guided memory. Nat. Neurosci. *19*, 992–994.

Selimbeyoglu, A., Kim, C.K., Inoue, M., Lee, S.Y., Hong, A.S.O., Kauvar, I., Ramakrishnan, C., Fenno, L.E., Davidson, T.J., Wright, M., and Deisseroth, K. (2017). Modulation of prefrontal cortex excitation/inhibition balance rescues social behavior in CNTNAP2-deficient mice. Sci. Transl. Med. *9*, eaah6733.

Sun, Q., Li, X., Ren, M., Zhao, M., Zhong, Q., Ren, Y., Luo, P., Ni, H., Zhang, X., Zhang, C., et al. (2019). A whole-brain map of long-range inputs to GABAergic interneurons in the mouse medial prefrontal cortex. Nat. Neurosci. *22*, 1357–1370.

Wall, N.R., Wickersham, I.R., Cetin, A., De La Parra, M., and Callaway, E.M. (2010). Monosynaptic circuit tracing in vivo through Cre-dependent targeting and complementation of modified rabies virus. Proc. Natl. Acad. Sci. U S A *107*, 21848–21853.

Walum, H., and Young, L.J. (2018). The neural mechanisms and circuitry of the pair bond. Nat. Rev. Neurosci. *19*, 643–654.

Yizhar, O., Fenno, L.E., Prigge, M., Schneider, F., Davidson, T.J., O'Shea, D.J., Sohal, V.S., Goshen, I., Finkelstein, J., Paz, J.T., et al. (2011). Neocortical excitation/inhibition balance in information processing and social dysfunction. Nature *477*, 171–178.

iScience, Volume *23*

Supplemental Information

Ventral Hippocampal-Prefrontal Interaction Affects Social Behavior via Parvalbumin Positive Neurons in the Medial Prefrontal Cortex

Qingtao Sun, Xiangning Li, Anan Li, Jianping Zhang, Zhangheng Ding, Hui Gong, and Qingming Luo

TRANSPARENT METHODS

KEY RESOURCES TABLE

REAGENT or RESOURCE	SOURCE	IDENTIFIER
Antibodies		
anti-PV	Millipore	MAB1572
anti-SST	santa cruz	sc-7819
anti-VIP	Millipore	AB982
Alexa Fluor 405,Gt-Anti-Mouse,H;	Invitrogen	A-31553
Alexa Fluor 647,Rb-Anti-Gt ,H+L;	Invitrogen	A-21446
Alexa Fluor 405,Gt-Anti-Rabbit,H.	Invitrogen	A-31556
Bacterial and Virus Strains		
AAV8-CAG -FLEx-glycoprotein	UNC Vector Core (Chapel Hill, NC)	Naoshige Uchida
AAV8- EF1a -FLEx-TVA-mCherry	UNC Vector Core (Chapel Hill, NC)	Naoshige Uchida
AAV2/9-EF1a-DIO-hCHR2(H134R)-mCherry	BrainVTA Co., Ltd., Wuhan, China	PT-0002
AAV2/9-EF1a-DIO-GCaMP6s	BrainVTA Co., Ltd., Wuhan, China	PT-0071
AAV2/9-CaMKII-NpHR3.0-YFP	BrainVTA Co., Ltd., Wuhan, China	PT-0008
SAD-ΔG-GFP(EnvA)-RV	BrainVTA Co., Ltd., Wuhan, China	R01001
SAD-ΔG-DsRed(EnvA)-RV	BrainVTA Co., Ltd., Wuhan, China	R01002
AAV2/9-EF1a-DIO-NpHR3.0-mCherry	BrainVTA Co., Ltd., Wuhan, China	PT-0007
RetroAAV-Cre	BrainVTA Co., Ltd., Wuhan, China	PT0136
AAV2/9- EF1a-fDIO-hChR2-mCherry	Taitool Bioscience Co. Ltd, Shanghai, China	S0404
AAV2/9- EF1a-DIO-hM4D(Gi)-mCherry	Taitool Bioscience Co. Ltd, Shanghai, China	S0193
AAV2/9- CaMKII-hM4D(Gi)-mCherry	Taitool Bioscience Co. Ltd, Shanghai, China	S0194
Chemicals, Peptides, and Recombinant Proteins		
PBS	Sigma-Aldrich	P3563
paraformaldehyde	Sigma-Aldrich	158127
Sucrose	Sigma-Aldrich	V900116
clozapine-n-oxide (CNO)	enzo lifesciences	BML-NS105-0005
Experimental Models: Organisms/Strains		
PV-Cre	Jackson Laboratory	008069
SST-Cre	Jackson Laboratory	013044
VIP-Cre	Jackson Laboratory	010908
PV-2A-Flpo	Jackson Laboratory	022730
C57BL/6	Hfkbio Co. Ltd, Beijing, China	
Software and Algorithms		

MATLAB	Mathworks, Inc.	https://www.mathworks.com
Graphpad prism 6.01	GraphPad Software	https://www.graphpad.com

CONTACT FOR REAGENT AND RESOURCE SHARING

All requests for resources should be directed to and will be fulfilled by Qingming Luo (qluo@mail.hust.edu.cn)

EXPERIMENTAL MODEL AND SUBJECT DETAILS

ANIMALS

PV-Cre (Madisen et al., 2010), SST-Cre, VIP-Cre (Taniguchi et al., 2011), PV-flpo (Madisen et al., 2015) and C57BL/6 adult male mice (2-3months) were used for virus tracing, optogenetics, chemogenetics and fiber photometry. In social discrimination test, juvenile male mice (<8 weeks) were used as novel targets. Mice were housed under 22 ± 1 °C and 55 ± 5% humidity with food and water ad libitum. Animal experiments were conducted in accordance with the Institutional Animal Ethics Committee of Huazhong University of Science and Technology.

VIRUS

The AAV8-CAG -FLEx-glycoprotein (Watabe-Uchida et al., 2012) (3.3×10^{12} gc/ml) and AAV8- EF1a -FLEx-TVA-mCherry (Watabe-Uchida et al., 2012) (8×10^{12} gc/ml) were purchased from the UNC Vector Core (Chapel Hill, NC). AAV2/9-EF1a-DIO-hCHR2(H134R)-mCherry(2×10^{12} gc/ml), AAV2/9-EF1a-DIO-GCaMP6s(2×10^{12} gc/ml), AAV2/9-CaMKII-NpHR3.0-YFP (2×10^{12} gc/ml), SAD-ΔG-GFP(EnvA)-RV(5×10^{8} IU/mL) and SAD-ΔG-DsRed(EnvA)-RV (5×10^{8} IU/mL), AAV2/9-EF1a-DIO-NpHR3.0-mCherry(2×10^{12} gc/ml), RetroAAV-Cre(5×10^{12} gc/ml) were purchased from BrainVTA (BrainVTA Co., Ltd., Wuhan, China). AAV2/9- EF1a-fDIO-hChR2-mCherry (2×10^{12} gc/ml), AAV2/9- EF1a-DIO-hM4D (Gi) -mCherry (2×10^{12} gc/ml), AAV2/9- CaMKII-hM4D(Gi)-mCherry(2×10^{12}gc/ml) were purchased from Taitool Bioscience (Taitool Bioscience Co. Ltd, Shanghai, China).

VIRUS INJECTIONS

For retrograde monosynaptic tracing, 150 nL viral cocktail(1:2) containing AAV8-EF1a -FLEx-TVA-mCherry and AAV8-CAG -FLEx-glycoprotein was injected into the prelimbic area(bregma1.9 mm, lateral 0.3 mm, depth 2.3 mm from skull surface) of PV-

Cre, SST-Cre and VIP-Cre mice. Three weeks later, 300-400 nL SAD-ΔG-GFP(EnvA)-RV or SAD-ΔG-DsRed(EnvA)-RV was injected into the same site.

For activation of GABAergic neurons in the mPFC, 300 nL AAV2/9-EF1a-DIO-hCHR2(H134R)-mCherry was injected into prelimbic area. For inhibition of vHIP, 400nl AAV2/9-CaMKII-NpHR3.0-YFP was injected into vHIP bilaterally (bregma-3.4mm, lateral ±3.5 mm, depth 4 mm from skull surface).

For fiber photometry, 300 nL AAV2/9-EF1a-DIO-GCaMP6s was injected into prelimbic area. The optical fiber (200 mm O.D., 0.37 numerical aperture (NA), Newdoon Inc. China;) was placed 300 μm above the virus injection sites. All the viruses were delivered by a sharp micropipette mounted on a Nanoject II(Drummond Scientific Co., Broomall, PA, USA) attached to a micromanipulator and then injected at a speed of 60 nL per min. The glass micropipette was held for an extra 10 min after the completion of the injection and then slowly retreated. After the surgery, the incisions were stitched and lincomycin hydrochloride and lidocaine hydrochloride gel was applied to prevent inflammation and alleviate pain for the animals. For optogenetics and fiber photometry, dental cement was used to fix the optical fibers.

For chemogenetics, 300 nL AAV2/9- EF1a-DIO-hM4D(Gi)-mCherry was injected into the vHIP of PV-flpo mice bilaterally, 300 nL viral cocktail (1:2) containing RetroAAV-Cre and AAV2/9- EF1a-fDIO-hChR2-mCherry was injected into the prelimbic area simultaneously. 300 nL AAV2/9- CaMKII-hM4D(Gi)-mCherry was injected into the vHIP of VIP-Cre mice bilaterally, 300 nLAAV2/9-EF1a-DIO-NpHR3.0-mCherry was injected into the prelimbic area simultaneously. After the virus injections, the optical fibers was planted into the prelimbic area with dental cement bilaterally for optogenetics manipulations.

HISTOLOGY

Mice were deeply anesthetized with sodium pentobarbital (1% wt/vol) and subsequently intracardially perfused with 0.01M PBS (Sigma-Aldrich Inc., St Louis, MO, USA), followed by 4% paraformaldehyde (Sigma-Aldrich Inc., St Louis, MO, USA) and 2.5% sucrose (Sigma-Aldrich Inc., St Louis, MO, USA) in 0.01M PBS. The brains were excised and post-fixed in 4% paraformaldehyde at 4°C for 12 h. For immunohistochemistry, the mouse brain was sectioned at 50μm on a vibration microtome (Leica, VT1200S). The sections of interests were blocked with 5%(wt/vol) BSA containing 0.3% Triton-X 100 (vol/vol) in 0.01 M PBS for 1 h, then incubated with the following primary antibodies (12 h at 4 °C):anti-PV(1:1000, mouse,

Millipore,MAB1572), anti-SST(1:200, goat, santa cruz, sc-7819), anti-VIP(1:100, rabbit, AB982). After rinsing, sections were incubated with following fluorophore-conjugated secondary antibody for 2 h at room temperature (1:400; Invitrogen): Alexa Fluor 405,Gt-Anti-Mouse,H; Alexa Fluor 647,Rb-Anti-Gt ,H+L; Alexa Fluor 405,Gt-Anti-Rabbit,H. Antibodies were diluted in the same block solution.

MICROSCOPY

For immunohistochemistry imaging, the sections were mounted by 50% glycerol (vol/vol) and imaged using a 20×, 0.75NA objective (Zeiss 710). For dual color RV imaging shown in Fig.1, the sections were mounted by 50% glycerol (vol/vol) and imaged using a 10×, 0.45NA objective (Olympus VS120 virtual microscopy slide scanning system, Olympus, Shanghai, China). For hippocampal axon terminal imaging, the brain slices containing mPFC area were imaged using a 40×, 1.4NA oil objective (Zeiss 710).

METHOD DETAILS

SOCIAL DISCRIMINATION TEST

The social discrimination test (SDT) procedures were similar to previous studies (Okuyama et al., 2016). Test mice were handled by the investigator for several minutes on each of two separate days (Day-1 and Day-2). The test mice were allowed to explore the social discrimination chamber (40 x 40 cm square, 30cm height) for ten minutes on Day-1 and Day-2 with pencil holders (circle with a radius of 7.5 cm and 15 cm height) placed at the upper right and lower left corners of social discrimination chamber. On day-3, the test mice were placed in social discrimination chamber, while the littermates and novel mice were kept in the pencil holders placed at the upper right and lower left corners of social discrimination chamber. The test mice were allowed to explore the chamber for 4 minutes before returned to home cages. Behavioral recordings and trackings were performed for 4 min by Ethovision XT software, using an infra-red (IR) sensitive GIG-E camera with two IR illuminators under dark conditions. On day-4, we used 570nm laser (20mW, persistent inhibition) to inhibit the activity of vHIP through optical fibers (Intelligent light system, Newdoon Inc. China) and repeated the same experimental procedure on Day-3. On Day-5, we used 470nm laser (15mW, 20Hz,15ms duration) to activate the GABAergic neurons in the mPFC and 570nm laser to inhibit the activity of vHIP simultaneously through optical fibers (Intelligent light system, Newdoon Inc. China) and repeated the same experimental procedure on Day-3. All the

light delivery were 1min later after the test mice entered the social discrimination chamber and last for 3 min. During SDT on day-3, day-4 and day-5, different novel mice was used to avoid the familiarization between the test mice and stimulus mice. The social interactions were manually scored when the test mice sniffed or climbed the pencil holders at the corners of social discrimination chamber while the travelling distance and speed were automatically calculated by Ethovision XT software.

For acute chemogenetics manipulations, PV-flpo mice and VIP-Cre mice that expressed hM4Di in their hippocampus were acclimated to IP needle pokes for one weeks prior to behavioral tests, though were not injected with any substance. On testing day, mice received a single IP injection of CNO (5mg/kg of body weight) 30min before testing. CNO was was dissolved in 0.9%(wt/vol) saline (5mg in 10ml). The control group received a single IP injection of 0.9%(wt/vol) saline instead of CNO. For blank control group, C57BL/6 mice were acclimated to IP needle pokes for one weeks prior to behavioral tests, though were not injected with any substance. On testing day, C57BL/6 mice received a single IP injection of CNO (5mg/kg of body weight) 30min before testing. After the behavior test, the mice were allowed to rest for 1h. Then the PV-flpo mice and VIP-Cre mice that received CNO injections were tested again. Different novel mice was used to avoid the familiarization between the test mice and stimulus mice. In the meantime, we used 470nm laser (15mW, 20Hz,15ms duration) to activate the $PV+_{mPFC}$ of PV-flpo mice and 570nm laser (20mW, persistent inhibition) to inhibit the $VIP+_{mPFC}$ (VIP+ neurons in mPFC) of VIP-Cre mice.

NOVEL/FAMILIAR OBJECT TEST

Mouse handling and habituation procedures were identical to SDT. On Day-1 and Day-2, The test mice were allowed to explore the chamber (40 x 40 cm square, 30cm height) for ten minutes with two table tennis ball (familiar object) put at the upper right and lower left corners of the chamber. On Day-3, the test mice were allowed to explore the chamber for five minutes with two table tennis ball (familiar object) put at the upper right and lower left corners of the chamber. Behavioral recording and tracking were performed for 5 min by Ethovision XT software, using an infra-red (IR) sensitive GIG-E camera with two IR illuminators under dark conditions. After the exploration, the test mice were returned to home cages to rest for ten minutes. Then the test mice explored the chamber again. The table tennis ball put at the upper right corners of the chamber was replaced by a small plastic cup (circle with a radius of 3.5 cm and 5 cm height) as novel object. The test mice were allowed to explore the chamber for five minutes before

returned to home cages. During the exploration, half of the test-mice were assessed under OFF-laser conditions while the other half received a counterbalanced protocol. Behavior recording conditions and laser conditions were identical to SDT. The object interactions were manually scored when the test mice sniffed or climbed the object at the corners of the chamber.

FIBER PHOTOMETRY

The fiber photometry procedures were similar to previous studies (Li et al., 2016, Wang et al., 2017). Fiber recordings were performed in freely moving mice three weeks after virus injection. To induce fluorescence signals, a laser beam from a laser tube (488 nm) was reflected by a dichroic mirror, focused by a 10x len (NA = 0.3) and then coupled to an optical commutator. A 3-m optical fiber (200 mm O.D., NA = 0.37) guided the light between the commutator and the implanted optical fiber. To minimize photo bleaching, the power intensity at the fiber tip was adjusted to 0.02 mW. The GCaMP6s fluorescence was band-pass filtered (MF525-39, Thorlabs) and collected by a photomultiplier tube (R3896, Hamamatsu). An amplifier (C7319, Hamamatsu) was used to convert the photomultiplier tube current output to voltage signals, which was further filtered through a low-pass filter (40 Hz cut-off; Brownlee 440). The analog voltage signals were digitalized at 100 Hz and recorded by a Power 1401 digitizer and Spike2 software (CED, Cambridge, UK). The calcium signals and the social interactions was simultaneously recorded by data acquisition software (Thinkertech, China) and the calcium data from each continuous experimental trial was normalized to the averaged fluorescence by a self-developed MATLAB program.

QUANTIFICATION AND STATISTICAL ANALYSIS

All statistical graphs were generated using Graphpad prism 6.01. The two-tailed paired, unpaired student's t test and one-way ANOVA were also performed using Graphpad prism 6.01. The AUC (area under curve) analysis was also performed using Graphpad prism 6.01. The confidence level was set to 0.05 (P value), and all results are presented as the means±s.e.m.

Reference:

Li, Y., Zhong, W., Wang, D., Feng, Q., Liu, Z., Zhou, J., Jia, C., Hu, F., Zeng, J., Guo, Q., Fu, L. & Luo, M. 2016. Serotonin neurons in the dorsal raphe nucleus encode reward signals. *Nat Commun,* 7**,** 10503.

Madisen, L., Garner, A. R., Shimaoka, D., Chuong, A. S., Klapoetke, N. C., Li, L., van der Bourg, A., Niino, Y., Egolf, L., Monetti, C., Gu, H., Mills, M., Cheng, A., Tasic,

B., Nguyen, T. N., Sunkin, S. M., Benucci, A., Nagy, A., Miyawaki, A., Helmchen, F., Empson, R. M., Knopfel, T., Boyden, E. S., Reid, R. C., Carandini, M. & Zeng, H. 2015. Transgenic mice for intersectional targeting of neural sensors and effectors with high specificity and performance. *Neuron,* 85**,** 942-958.

Madisen, L., Zwingman, T. A., Sunkin, S. M., Oh, S. W., Zariwala, H. A., Gu, H., Ng, L. L., Palmiter, R. D., Hawrylycz, M. J., Jones, A. R., Lein, E. S. & Zeng, H. 2010. A robust and high-throughput Cre reporting and characterization system for the whole mouse brain. *Nat Neurosci,* 13**,** 133-140.

Okuyama, T., Kitamura, T., Roy, D. S., Itohara, S. & Tonegawa, S. 2016. Ventral CA1 neurons store social memory. *Science,* 353**,** 1536-1541.

Taniguchi, H., He, M., Wu, P., Kim, S., Paik, R., Sugino, K., Kvitsani, D., Fu, Y., Lu, J. T., Lin, Y., Miyoshi, G., Shima, Y., Fishell, G., Nelson, S. B. & Huang, Z. J. 2011. A Resource of Cre Driver Lines for Genetic Targeting of GABAergic Neurons in Cerebral Cortex. *Neuron,* 71**,** 995-1013.

Wang, D., Li, Y., Feng, Q., Guo, Q., Zhou, J. & Luo, M. 2017. Learning shapes the aversion and reward responses of lateral habenula neurons. *Elife,* 6.

Watabe-Uchida, M., Zhu, L., Ogawa, S. K., Vamanrao, A. & Uchida, N. 2012. Whole-brain mapping of direct inputs to midbrain dopamine neurons. *Neuron,* 74**,** 858-873.

Supplementary Figure

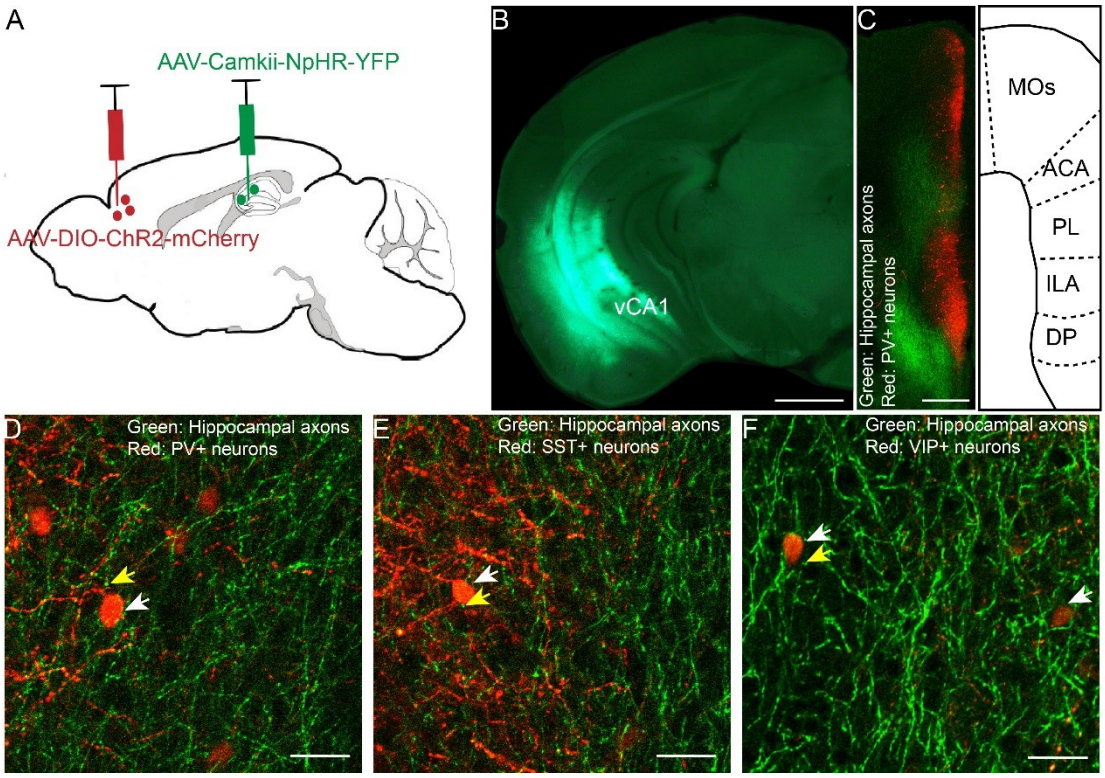

Supplementary Figure 1 Different GABAergic neurons in mPFC are innervated by hippocampal axons, related to figure 1.

A. Schematic of the experimental strategy to label different GABAergic neurons and hippocampal axons in mPFC. AAV-DIO-ChR2-mCherry was injected into the mPFC of different Cre driver lines to label different GABAergic neurons while the AAV-Camkii-NpHR-YFP was injected into the ventral hippocampus to label the hippocampal axons in mPFC. B,C. Injection sites at the ventral hippocampus and mPFC. D-F. Different GABAergic neurons in mPFC are heavily innervated by hippocampal axons. The white arrows showed the GABAergic neurons in mPFC that are surrounded by hippocampal axons. The yellow arrows showed the boutons of hippocampal axons. Scale bar in B is 1mm. Scale bar in C is 500μm. Scale bars in D-F are 30μm.

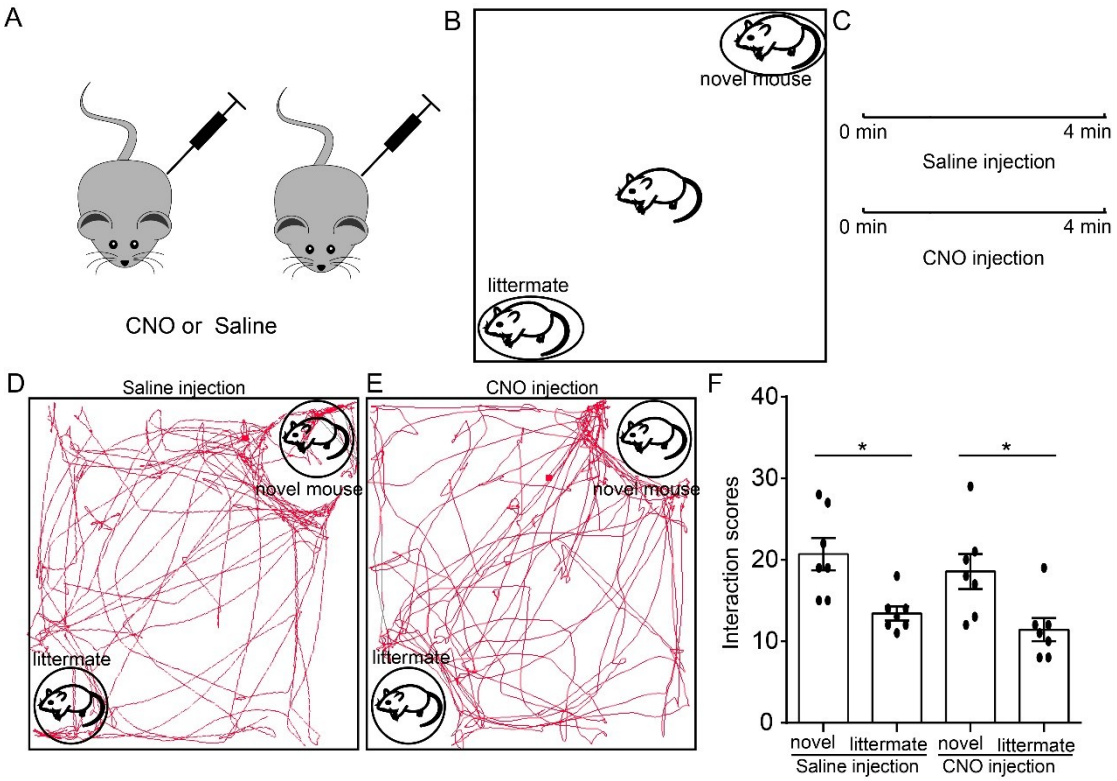

Supplementary Figure 2 Administration of CNO alone did not affect social behavior, related to figure 5 and 6.

A. C57BL/6 mice was injected intraperitoneally with CNO or saline. B. Experimental strategy of social discrimination test. C. Timeline of social discrimination test. D, E. Position tracking from representative mice during social discrimination test with CNO injection or saline injection. F. Social interaction times with novel mice or littermates with different experimental conditions.(Paired t-test, *$p<0.05$)